UNIVERSITY OF SPLIT

**FACULTY OF ELECTRICAL ENGINEERING,
MECHANICAL ENGINEERING AND NAVAL ARCHITECTURE**

POSTGRADUATE DOCTORAL STUDIES MECHANICAL ENGINEERING

QUALIFYING EXAM

A Review of Digital Image Correlation and Infrared Thermography with Perspectives on Data-Driven Full-Field Reconstruction

Alen Grebo

Split, July 2026

Table of Contents:

1. Introduction

Full-field experimental measurement techniques play an increasingly important role in modern experimental mechanics, as they provide detailed insight into material behaviour and structural response under mechanical loading. In contrast to conventional point-based sensors, such as strain gauges or thermocouples, full-field approaches offer spatially continuous information over an entire region of interest. An example of full-field Digital Image Correlation (DIC) performed on a three-point bending test can be seen in Figure 1.1. DIC enables the observation of heterogeneous deformation, strain localisation, and damage initiation, which are often decisive for understanding complex mechanical phenomena. Such information is particularly relevant when studying advanced materials, advanced structures, or systems subjected to non-linear and dynamic loading, where local effects frequently govern the global response [1]. Although traditional contact-based measurement techniques remain widely used due to their robustness and simplicity, they exhibit inherent limitations. Measurements are restricted to discrete locations and may therefore fail to capture highly localised effects such as crack initiation, plastic zone evolution, or rapid strain redistribution. Furthermore, contact sensors may influence the mechanical response of lightweight structures or small-scale specimens. These limitations have motivated the growing adoption of non-contact optical and thermal measurement techniques capable of providing full-field data with high spatial resolution.

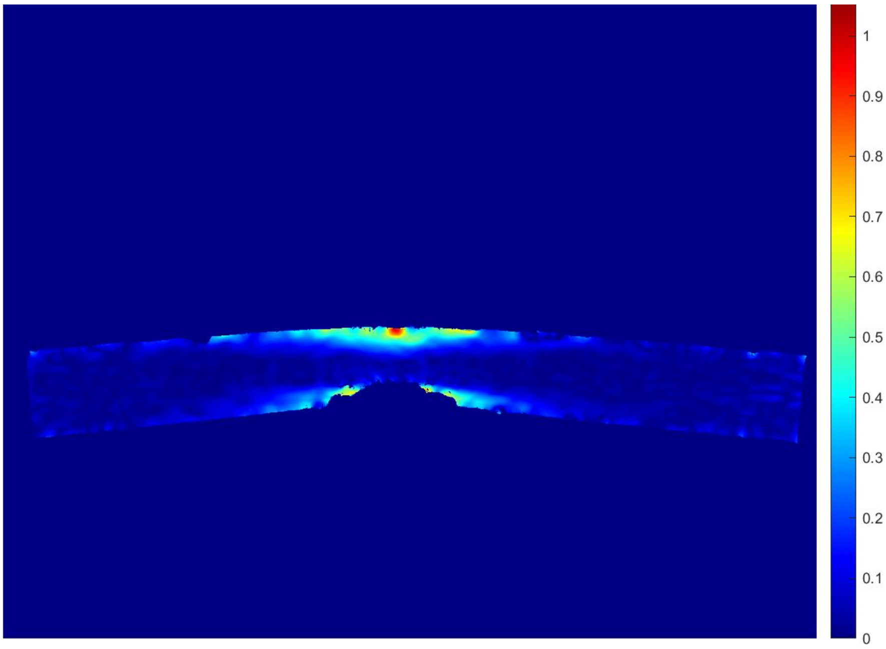

Figure 1.1. Full-field effective strain distribution of a three-point bending sample obtained using Digital Image Correlation (DIC).

Digital Image Correlation (DIC) has become one of the most established optical techniques for full-field displacement and strain measurement [2]. The method is based on tracking the deformation of a random surface pattern by correlating digital images acquired during mechanical loading. By comparing images recorded in the reference and deformed states, DIC enables accurate, non-contact measurement of in-plane and out-of-plane displacements. Due to its flexibility and relatively straightforward experimental implementation, DIC has been applied across a wide range of length scales, from micro-mechanical testing to large-scale structural experiments (see Figure 1.2.) [1,2,3]. Nevertheless, the accuracy of DIC measurements depends strongly on image quality, surface preparation, and correlation parameters, and may deteriorate under challenging experimental conditions [2].

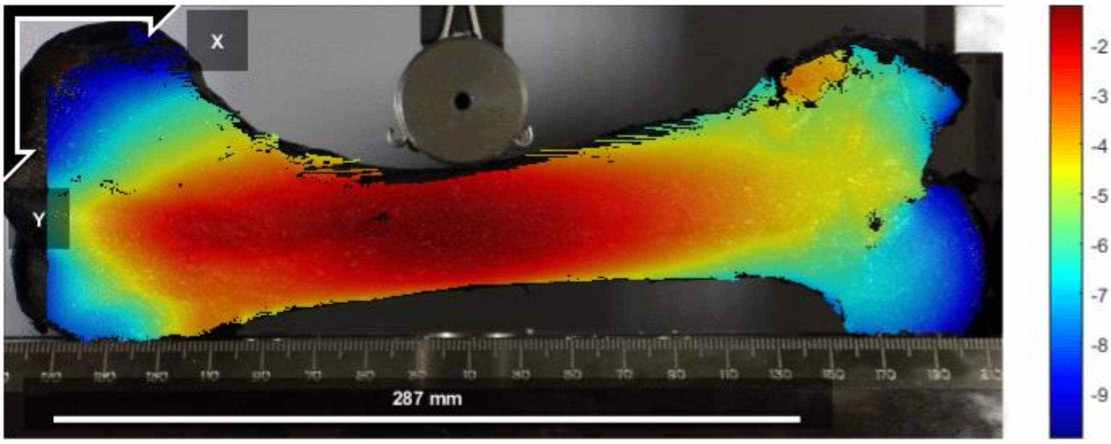

a)

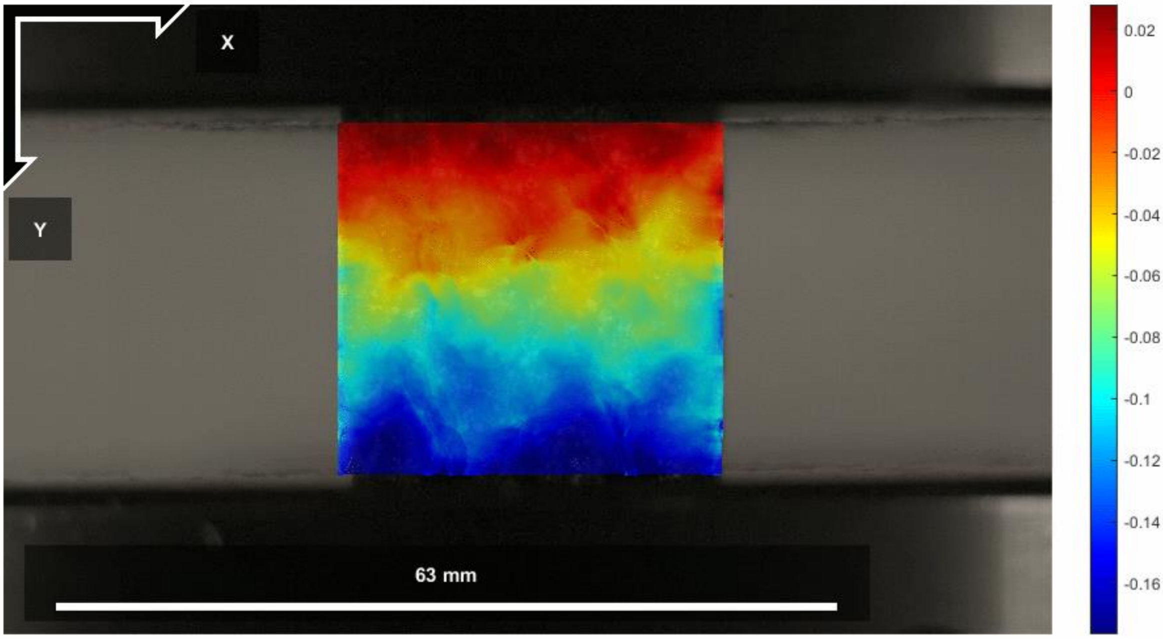

b)

Figure 1.2. Effective (equivalent) strain fields measured using Digital Image Correlation (DIC): a) full-field distribution over a bone specimen; b) localised strain field within a defined region of interest, illustrating deformation localisation and strain gradients.

Infrared Thermography (IRT) provides a complementary full-field measurement technique by capturing thermal responses associated with mechanical loading (see Figure 1.3.). By detecting infrared radiation emitted from a surface, IRT enables non-contact monitoring of temperature fields and their temporal evolution. In experimental mechanics, thermal signals can be related to underlying mechanical processes such as elastic deformation through the thermoelastic effect, as well as irreversible phenomena including plastic deformation, friction, and damage-related heat generation [4,5,6]. As a result, Infrared Thermography has found broad application in material characterisation, non-destructive testing, and structural health monitoring. However, thermal measurements are influenced by surface emissivity, environmental radiation, and camera characteristics, which may limit both spatial resolution and measurement accuracy [6].

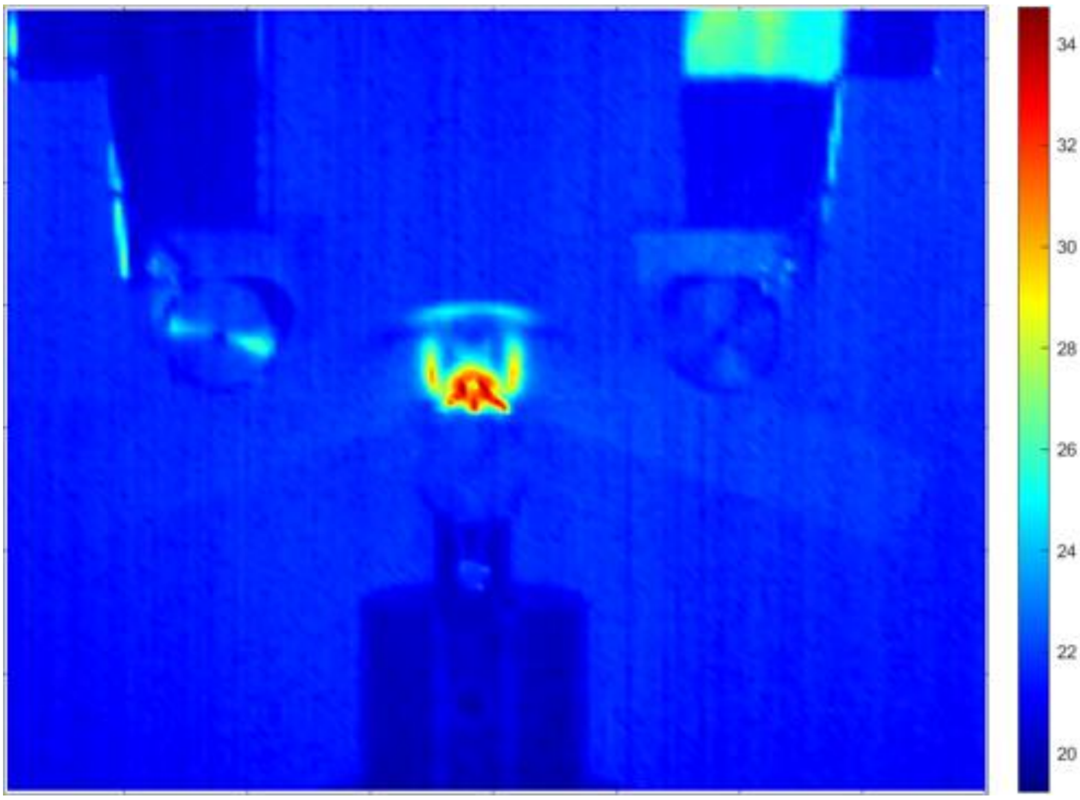

Figure 1.3. Localised temperature increases in the region of deformation during mechanical loading acquired via Infrared Thermography.

The use of infrared thermography becomes particularly challenging in dynamic and high-speed mechanical testing. Short event durations and high loading rates impose strict requirements on temporal resolution, often necessitating the use of cooled high-speed infrared cameras. Compared to standard systems, such cameras typically exhibit reduced spatial resolution, increased noise levels, and limited thermal sensitivity. Temperature changes associated with elastic and early plastic deformation are generally minimal and may not be reliably detected by infrared cameras (see Figure 1.4.), especially under high-speed loading conditions. High-speed motion can introduce artefacts in thermographic data, including image blur, pixel misregistration, and spurious temperature variations, while non-uniform emissivity may result in incorrect temperature measurements [7,8].

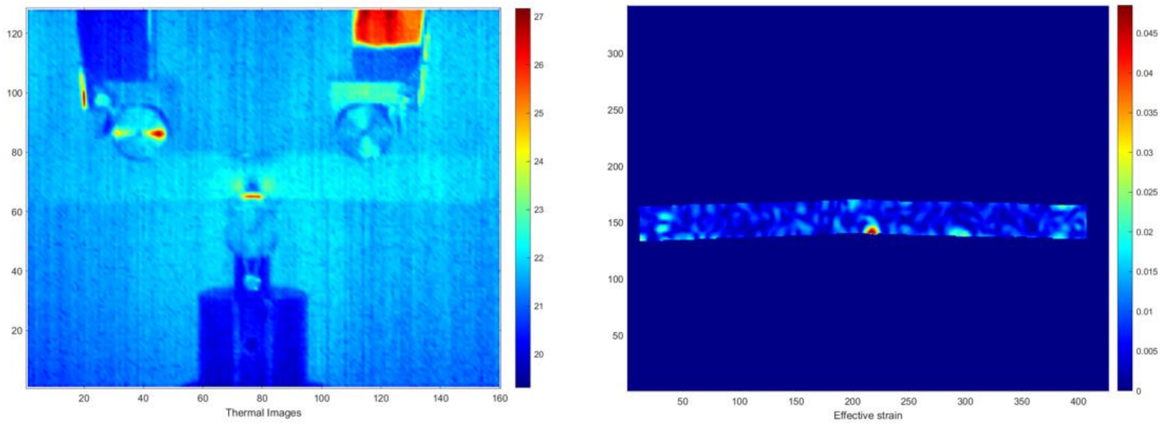

a) b)

Figure 1.4. Infrared and DIC response in the elastic regime: a) negligible temperature change due to thermoelastic effects; b) corresponding low-level effective strain field, illustrating deformation without significant energy dissipation

In addition to acquisition-related challenges, experimental safety requirements may fundamentally restrict the applicability of infrared thermography. In impact and high-energy tests, the region of interest is frequently enclosed within protective casings or shielding structures to prevent damage to optical equipment and ensure operator safety. These protective enclosures are commonly manufactured from materials that are opaque [9] in the infrared spectrum, thereby completely blocking thermal radiation emitted from the specimen surface. As a result, direct infrared measurements of the impact zone become impossible, regardless of camera sensitivity or acquisition speed. Even when partial infrared access is available, reflections, transmissivity losses, and additional noise sources may further degrade measurement reliability [7,10].

Further experimental complexity arises from the investigation of unconventional mechanical structures, such as auxetic and energy-absorbing cellular systems [11]. These structures exhibit non-classical deformation mechanisms, including negative Poisson's ratio behaviour [12], large local rotations, and highly non-uniform strain fields. Their mechanical response under static, dynamic, or impact loading is governed by a strong interplay between geometry, material behaviour, and deformation mode. Previous studies have shown that auxetic structures can provide enhanced energy dissipation and improved impact resistance compared to conventional designs; however, their complex and localised deformation patterns pose significant challenges for experimental characterisation using optical and thermal techniques [11,12]. When such complex structures are tested under dynamic conditions and enclosed within infrared-opaque [9] protective casings, the comprehensive assessment of their thermomechanical behaviour becomes particularly demanding. Limited measurement accessibility, rapid deformation, and strong coupling between kinematic and thermal responses often lead to incomplete or unreliable experimental observations. These constraints highlight the need for alternative strategies capable of compensating for missing or inaccessible information while retaining physical relevance.

Recent advances in artificial intelligence, particularly in deep learning, have introduced new possibilities for the analysis and interpretation of full-field experimental data. Convolutional neural networks have demonstrated strong performance in image-based tasks such as feature extraction (i.e. identifying local patterns such as edges, textures, and deformation structures), pattern recognition, and image-to-image regression [13,14]. These capabilities make deep learning approaches well suited for learning complex, non-linear relationships between different types of full-field measurements [15,16]. Within experimental mechanics, artificial intelligence has increasingly been explored for displacement and strain estimation [17], noise reduction, damage detection, and the prediction of mechanical or thermal fields from indirect observations [15,17,18,19].

The integration of artificial intelligence with full-field experimental techniques represents a promising pathway for addressing the practical limitations of individual measurement methods. By learning correlations between kinematic and thermal responses, data-driven models may act as surrogate representations capable of reconstructing thermal fields when direct infrared measurements are unreliable or fundamentally impossible. This approach is particularly relevant in dynamic and impact testing of complex structures, where experimental constraints severely limit direct access to thermomechanical information. At the same time, challenges related to data dependency, generalisation capability, and interpretability remain important considerations [20].

This paper provides a structured review of three core domains: digital image correlation, infrared thermography, and artificial intelligence-based image analysis. By reviewing the fundamental principles, applications, and limitations of each domain, this qualification study establishes the scientific background and motivation for considering artificial intelligence-driven approaches to full-field data fusion in experimental mechanics.

2. Motivation for AI-Based Data Fusion

The analysis of material behaviour in experimental mechanics increasingly relies on full-field measurement techniques capable of capturing spatially resolved mechanical and thermal responses. Among these, digital image correlation (DIC) and infrared thermography (IRT) are particularly valuable because they provide complementary information on deformation and temperature evolution, respectively. DIC enables accurate measurement of displacement and strain fields, while IRT provides access to thermal signatures associated with thermoelastic effects, plastic dissipation, and damage processes. Despite their individual strengths, these techniques are most often applied and interpreted separately, which limits the ability to describe the underlying thermomechanical behaviour in a unified manner.

This separation becomes particularly restrictive when studying deformation processes that are strongly coupled to heat generation. In many loading scenarios, especially those involving plasticity, localisation, or damage, mechanical work is partially converted into heat, meaning that strain and temperature fields evolve together rather than independently. As a result, the mechanical field measured by DIC and the thermal field measured by IRT represent two different manifestations of the same physical process. When analysed separately, part of this relationship remains hidden, and the interpretation of deformation and energy dissipation may therefore remain incomplete.

Artificial intelligence offers a possible way to bridge this gap. Recent studies have shown that convolutional and encoder–decoder networks can learn mappings between image-like fields, making them suitable for multimodal full-field data analysis. In DIC, deep learning has already been used for direct displacement and strain estimation, denoising, and correction of correlation-related errors [17,21,22,23]. In thermography, deep learning has been applied to defect detection, thermal pattern analysis, and interpretation of complex thermal data [18,19,24,25]. These developments indicate that full-field measurements can be treated as structured data, and that relationships between different physical fields may be learned directly from experiments.

Within this context, AI-based data fusion becomes a particularly relevant research direction. Rather than treating DIC and IRT as independent techniques, a data-driven framework can be used to establish a direct relationship between the two. Such a framework makes it possible to infer thermal behaviour from mechanical fields, or to interpret thermal observations in relation to the corresponding deformation state. This is especially relevant in situations where one modality is experimentally limited, noisy, or partially unavailable. The possibility of learning a mapping between strain and temperature fields therefore provides not only a new analysis tool, but also a means of extending the practical capabilities of experimental mechanics.

At the same time, such approaches remain challenging. The coupling between deformation and temperature is influenced by material behaviour, strain rate, geometry, boundary conditions, and heat transfer effects, making it difficult to describe through purely analytical models in complex experiments. Data-driven approaches can address this by learning directly from observations, but their success depends strongly on the availability of representative paired datasets and on the physical consistency of the learned mapping. For this reason, recent developments in physics-informed and hybrid machine learning are particularly relevant, as they aim to improve generalisation and preserve compatibility with governing physical relationships [26,27,28].

Although artificial intelligence has already been successfully applied to DIC and IRT separately, studies that directly couple these two full-field modalities within a unified data-driven framework remain limited. This gap highlights the relevance of reviewing AI-based data fusion approaches for linking mechanical fields obtained from DIC and thermal fields measured by IRT. Such approaches may support the interpretation of thermomechanical relationships that are difficult to access using either technique alone.

In summary, the motivation for AI-based data fusion arises from the need to move beyond separate analysis of mechanical and thermal measurements toward a more integrated description of material behaviour. Combining DIC, IRT, and deep learning provides a promising route for achieving this, particularly in the study of deformation localisation, energy dissipation, and complex thermomechanical responses.

3. Digital Image Correlation (DIC)

Digital Image Correlation (DIC) is a non-contact optical measurement technique used to obtain full-field displacement and strain information on the surface of deforming objects. By analysing sequences of digital images acquired during mechanical loading, DIC enables experimental characterisation of deformation patterns, strain localisation, and damage evolution with high spatial resolution. Due to its versatility and material-independent nature, the technique has become widely adopted in experimental mechanics across a broad range of applications and length scales, including metals, polymers, composites, concrete, biological materials, and designed cellular structures [1,2,29]. A key advantage of digital image correlation over traditional point-based measurement techniques, such as strain gauges or extensometers, lies in its ability to provide spatially continuous, full-field information. In addition, DIC is a non-contact measurement method, meaning that it does not introduce additional mass or stiffness into the system and therefore does not affect the dynamic response of the specimen through added inertia. This capability allows detailed investigation of heterogeneous deformation phenomena that are often inaccessible to discrete sensors, particularly in cases involving complex geometries, large deformations, or highly localised mechanical responses (see Figure 3.1.) [5,11,12,30].

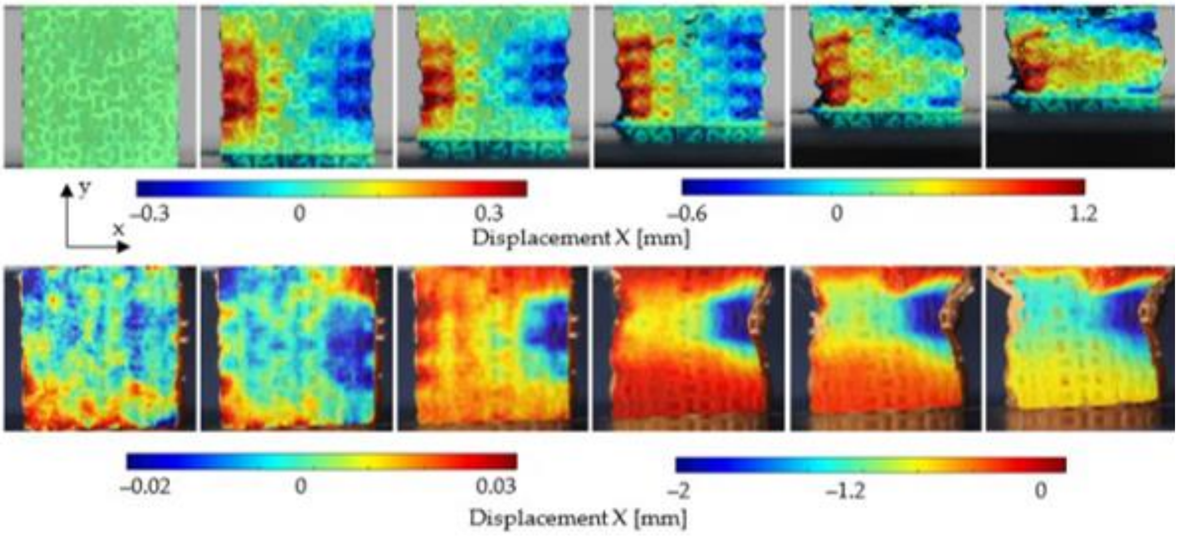

Figure 3.1. DIC-derived displacement field evolution of two auxetic structures: a) X-direction displacement maps showing progressive deformation; b) displacement evolution highlighting localisation and deformation mechanisms during loading [31].

Depending on experimental requirements, DIC may be implemented using a single-camera configuration for planar deformation measurements (2D-DIC) or a multi-camera stereo configuration to reconstruct three-dimensional surface kinematics [2,30]. Over the past two decades, the method has evolved from a laboratory-scale research tool into a recognised experimental technique, supported by extensive methodological developments, standardisation efforts, and a growing ecosystem of commercial and open-source software implementations [29,30,32].

In parallel with methodological advances, increasing emphasis has been placed on openness, reproducibility, and community-driven development in DIC research. Publicly available datasets, open-source software frameworks, and dedicated community platforms have been introduced to facilitate benchmarking of correlation algorithms, validation of numerical models, and transparent comparison of experimental results across research groups [30,32,33,34,35,36].

3.1. Fundamental Principles of Digital Image Correlation

The fundamental principle of digital image correlation assumes that the grey-level intensity pattern observed on the surface of a specimen remains conserved during deformation. Under this assumption, corresponding tracking points in reference and deformed images can be identified by analysing changes in the spatial distribution of image intensity values (see Figure 3.3.). This concept was first formalised in early developments of the method and has since formed the foundation of modern full-field optical deformation measurement techniques [1,2].

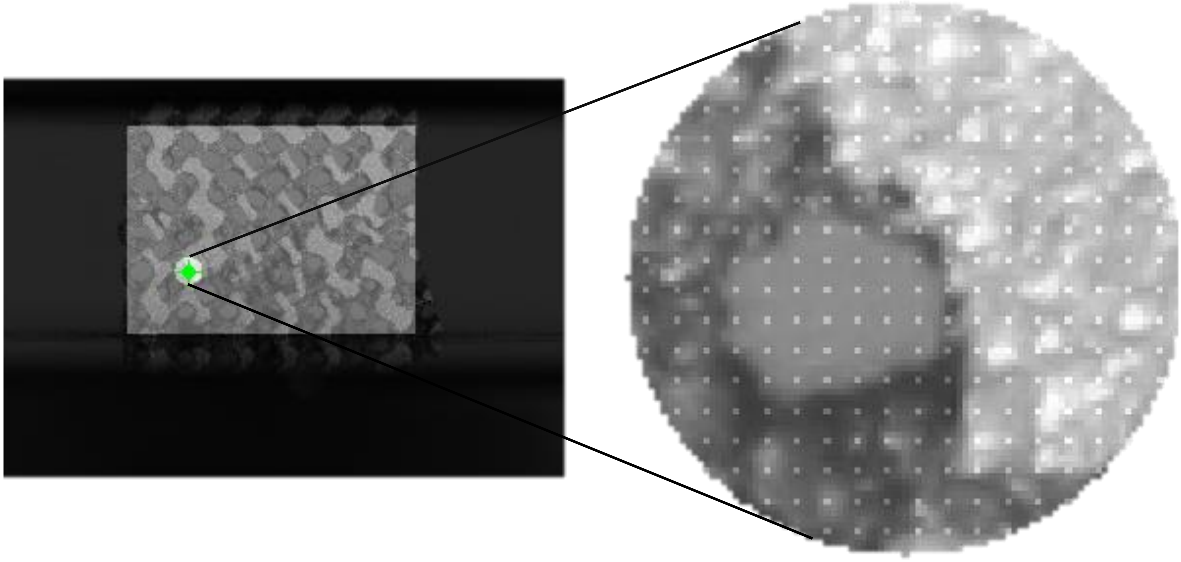

(a) (b)

Figure 3.2. Example of subset selection in digital image correlation. a) Region of interest on the specimen with a selected subset (green marker). b) Enlarged view of the subset, illustrating the speckle pattern used for tracking. Accurate correlation requires subsets with sufficiently unique intensity distributions to ensure reliable matching between images.

In a typical DIC analysis, a reference image of the undeformed specimen is first acquired, and the region of interest is discretised into small regions known as subsets (see Figure 3.2. and Figure 3.3.). For each subset in the reference image, the corresponding location in the deformed image is determined by maximising/minimising a correlation criterion that quantifies the similarity between the two image regions. Early implementations employed iterative optimisation schemes, such as Newton–Raphson-based partial differential correction [37], to achieve sub-pixel displacement accuracy (i.e. the ability to resolve displacements smaller than the physical pixel size of the image), forming the foundation of modern correlation algorithms [1,3,29,32,33,34].

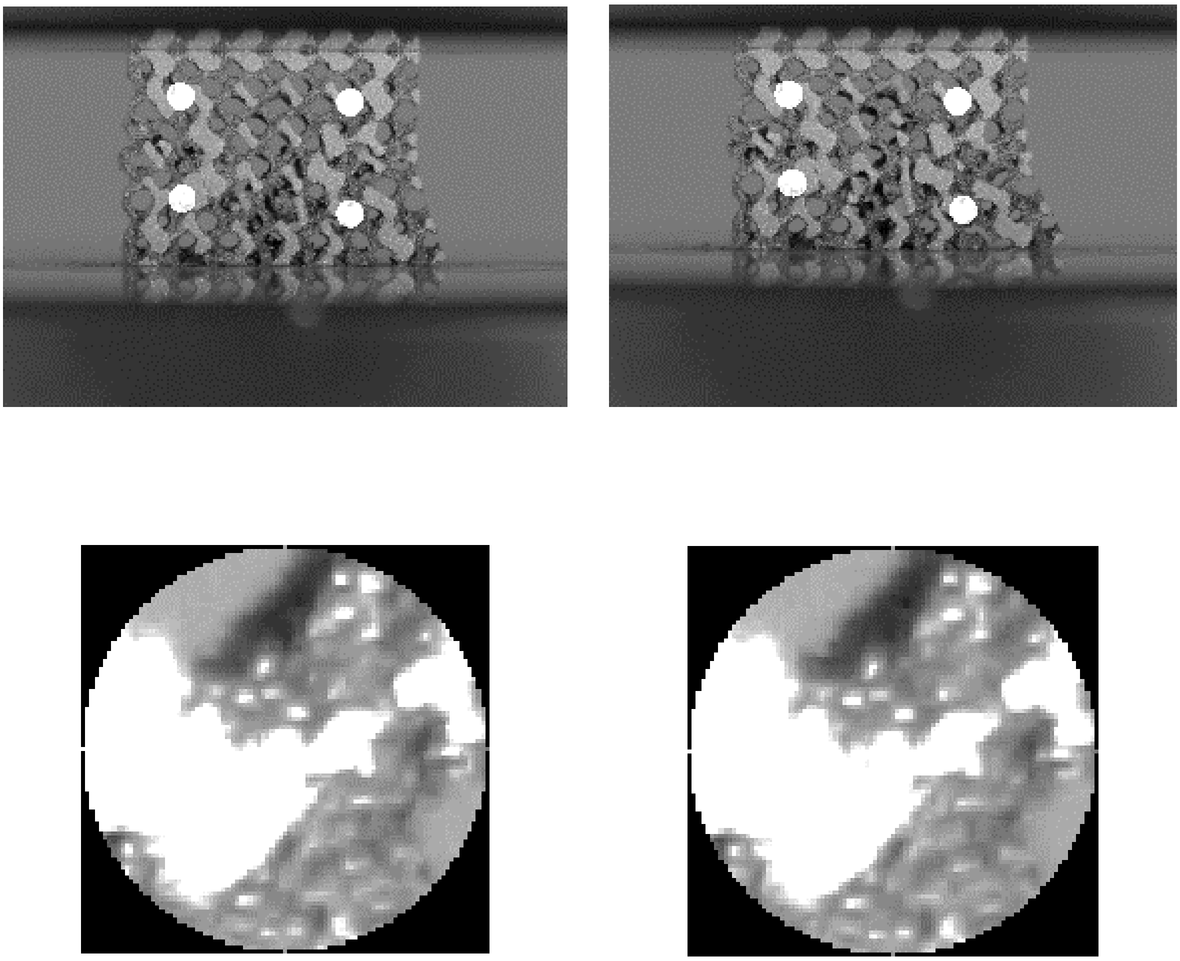

a) b)

Figure 3.3. Example of reference and deformed subsets used in Digital Image Correlation: (top) reference and deformed images with selected subset locations; (bottom) corresponding subset regions illustrating grayscale pattern deformation. a) Reference subset; b) Deformed subset.

To achieve sub-pixel displacement resolution (i.e. the ability to measure displacements smaller than the physical pixel spacing of the image), the grey-level intensity values within subsets are interpolated and iterative optimisation schemes are used to refine the displacement estimate. While this approach enables high measurement precision, the choice of interpolation scheme and subset formulation can introduce systematic errors [30], such as bias due to interpolation inaccuracies, sensitivity to image noise, and errors arising from an inadequate representation of deformation within the subset (e.g. insufficient shape functions) [1,2,3,29,38,39].

3.2. Image Acquisition and Speckle Patterns

Reliable DIC measurements require a suitable surface texture that allows unique identification of subsets during deformation. In many applications, a random, high-contrast speckle pattern is applied to the specimen surface using paint, ink, or other deposition techniques. The pattern must deform consistently with the underlying material and remain stable throughout the experiment. If the applied pattern is not sufficiently dry or properly bonded to the surface, it may peel or detach during high-deformation tests, leading to loss of correlation and unreliable measurements [30]. In addition to conventional visible-light speckle patterns (see Figure 3.4. - a), alternative approaches based on UV-sensitive paints combined with ultraviolet illumination (see Figure 3.4. – b) may be employed to enhance contrast and pattern stability under challenging experimental conditions [31]. Unlike conventional speckle patterns, which rely on reflected light, UV-sensitive particles emit light when excited, enabling the use of smaller and finer speckle features. This can improve spatial resolution and correlation quality by providing more distinct and densely distributed tracking points. Such approaches are particularly advantageous in situations where conventional illumination is limited or when multiple optical measurement techniques are used simultaneously, provided that the UV-responsive pattern remains well bonded and deforms consistently with the specimen surface.

a)

b)

Figure 3.4. Surface patterns for Digital Image Correlation: (a) conventional reflective speckle pattern; (b) UV-emitting speckle pattern under ultraviolet light, allowing finer speckle features and improved correlation performance [31].

The quality of the speckle pattern has a direct influence on correlation accuracy, spatial resolution, and measurement uncertainty. Systematic studies have demonstrated that speckle size, contrast, and spatial distribution strongly affect correlation performance, and that each subset should contain multiple distinct speckle features with sufficient grey-level variation [2,40].

Image acquisition parameters, including camera resolution, lens quality, depth of field, exposure time, and illumination uniformity, also play a crucial role in DIC performance. Stable and uniform illumination is particularly important, as variations in lighting conditions can violate the grey-level conservation assumption and introduce systematic errors. In dynamic experiments, high-speed imaging may be required, leading to trade-offs between temporal resolution, image noise, and spatial resolution [30].

3.3. Subset-Based (Local) Digital Image Correlation

Local, subset-based digital image correlation represents the most widely used formulation of the method and constitutes the primary focus of this work [2,29]. In local DIC, displacement is estimated independently for each subset (see Figure 3.5.), without enforcing global continuity of the displacement field, which distinguishes it from global and integrated formulations [36,41].

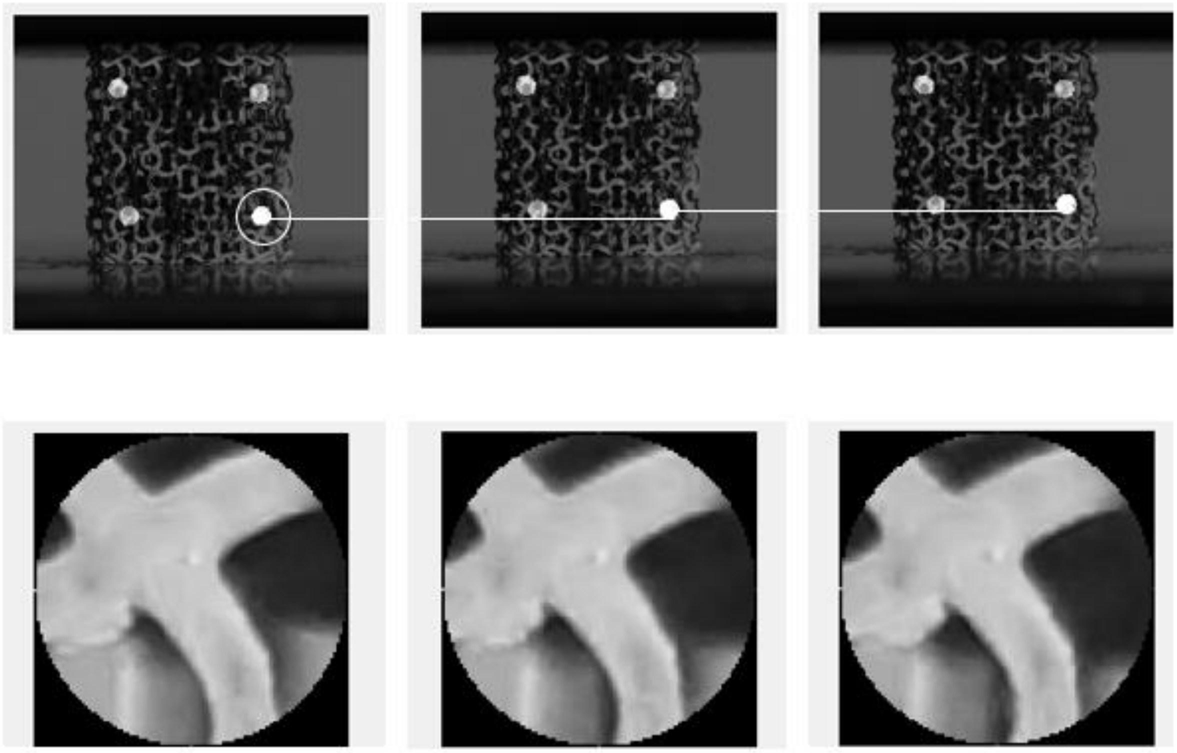

Figure 3.5. Subset tracking in digital image correlation across multiple time steps: (top row) sequential images showing the approximate subset location during deformation; (bottom row) corresponding subsets illustrating intensity pattern evolution used for displacement estimation.

This formulation provides a high degree of flexibility and allows the method to accommodate large deformations, strong strain gradients, and highly localised deformation phenomena, including crack initiation and propagation, which are difficult to capture using globally constrained approaches [29,42]. Owing to the independent treatment of subsets, local DIC has been shown to perform robustly in applications involving heterogeneous materials and complex deformation modes [36].

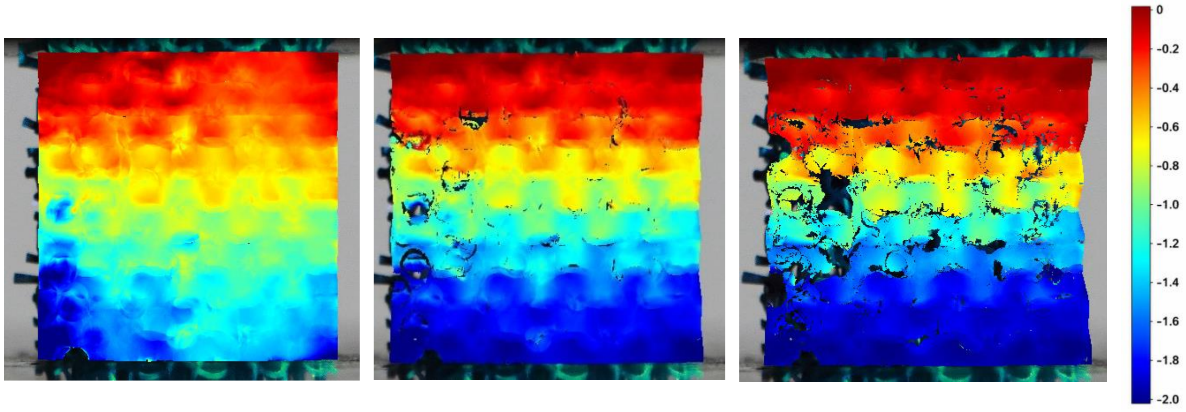

Figure 3.6. Vertical displacement (v) field obtained using digital image correlation for an auxetic structure, showing deformation evolution across successive loading stages [31].

In local DIC, displacement is estimated independently for each subset by tracking its motion between the reference and deformed images (see Figure 3.6. and Figure 3.7.), without enforcing continuity between neighbouring regions. Strain is subsequently obtained through spatial differentiation of the displacement field (see Figure 3.7. c, d, and e). This separation enables the displacement field to retain high spatial resolution, allowing accurate representation of heterogeneous deformation, including strong gradients and localised phenomena that could otherwise be suppressed by imposed continuity constraints [2]. However, the lack of global constraints increases sensitivity to image noise, particularly during strain computation, since numerical differentiation amplifies measurement uncertainty [2,3]. Consequently, smoothing, filtering, or regularisation techniques are typically required to obtain physically meaningful strain fields while preserving an appropriate balance between noise reduction and spatial resolution [29,36].

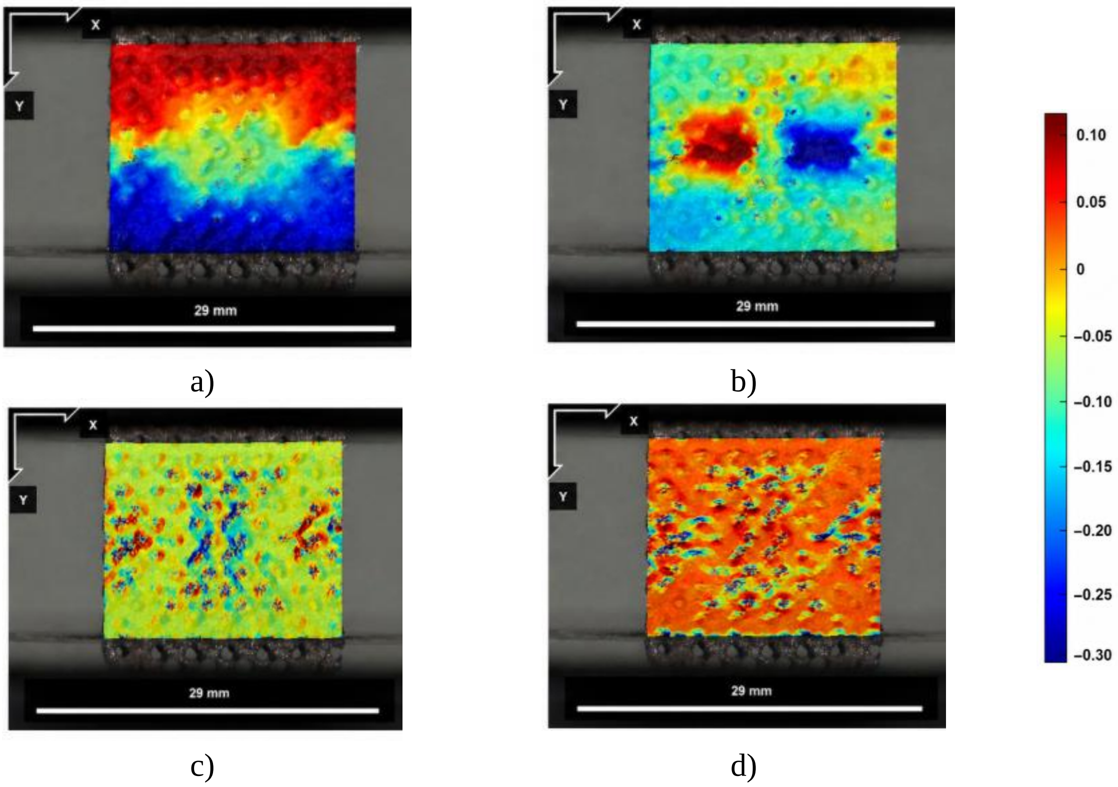

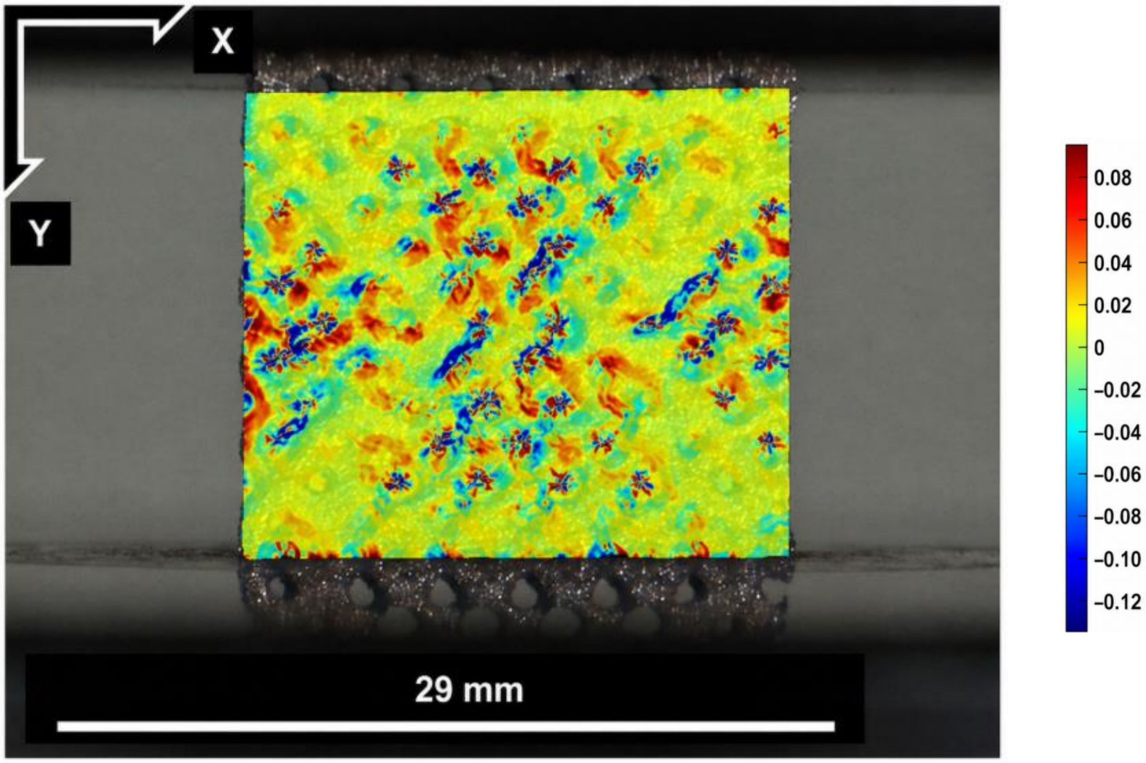

e)

Figure 3.7. Full-field displacement and strain maps obtained using digital image correlation: a) vertical displacement v; b) horizontal displacement u; c) normal strain εxx; d) normal strain εyy; and e) shear strain εxy.

The widespread availability of open-source subset-based DIC implementations has significantly contributed to the adoption of local DIC in experimental mechanics. Software such as NCorr [33] and pyDIC [34] provides transparent access to correlation parameters and processing workflows, while more general frameworks such as OpenCorr [43] and DICe [32] support extensible algorithm development and benchmarking. These characteristics make local DIC particularly well suited for research-oriented applications and for integration with numerical simulations and data-driven analysis methods.

3.4. Global and Integrated Digital Image Correlation

In contrast to local, subset-based approaches, global digital image correlation formulations estimate the displacement field over the entire region of interest simultaneously by expressing it in terms of global shape functions. These shape functions are most commonly derived from finite element discretisation, allowing the displacement field to be represented using continuous basis functions defined over the full measurement domain [2,36]. This formulation inherently enforces displacement continuity across the region of interest and has been shown to improve robustness to image noise compared to local correlation strategies (see Figure 3.8.) [41].

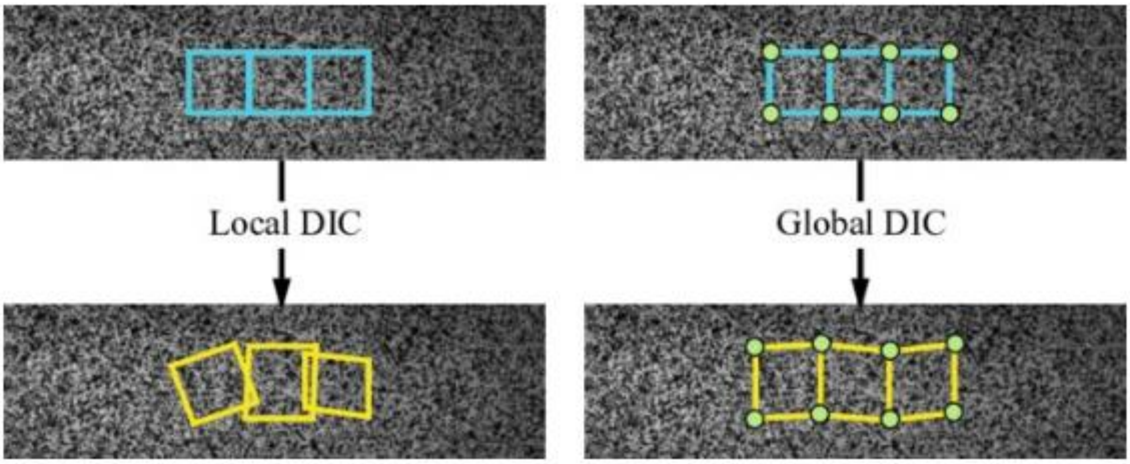

a) b)

Figure 3.8. Illustration of local and global DIC approaches [35].

Global DIC approaches solve the correlation problem as a single optimisation task, in which the unknown coefficients of the global shape functions [44] are determined by minimising the discrepancy between reference and deformed images. Because the displacement field is constrained by the chosen basis functions, global methods typically exhibit improved noise filtering properties but reduced flexibility when representing sharp displacement gradients or discontinuities [2,36].

Integrated digital image correlation extends global formulations by directly incorporating mechanical models into the correlation process. In these approaches, the displacement field is constrained not only by global shape functions but also by constitutive relations and equilibrium equations, enabling simultaneous identification of displacement fields and material parameters from image data [36,41]. While integrated DIC provides a physically consistent framework and enhanced noise robustness, its performance depends strongly on the validity of the assumed mechanical model [36,41].

Comparative studies have demonstrated that although global and integrated DIC approaches offer advantages in terms of noise sensitivity and physical consistency, local DIC remains more suitable for problems involving displacement discontinuities, strong strain localisation, and complex deformation mechanisms [36,41]. Consequently, the choice between local and global formulations should be guided by deformation characteristics, experimental objectives, and modelling assumptions rather than by methodological preference alone [30].

In the present review, global and integrated DIC approaches (see Figure 3.8.) are discussed for completeness, while the emphasis remains on local DIC due to its flexibility and suitability for capturing heterogeneous and highly localised deformation fields.

Beyond conventional surface-based approaches, correlation-based methods have also been extended toward volumetric measurements through Digital Volume Correlation (DVC). Unlike standard Digital Image Correlation, which measures deformation on the specimen surface, DVC enables measurement of internal displacement and strain fields using volumetric image data, most commonly obtained from X-ray computed tomography. Buljac et al. [45,46] describe DVC as an extension of Digital Image Correlation to volumetric image analysis, enabling investigation of internal deformation mechanisms that cannot be captured using surface measurements alone. Such approaches are particularly useful for the analysis of complex materials and structures exhibiting heterogeneous internal deformation, damage evolution, and strain localisation. Applications of DVC have been reported in the investigation of fibre-reinforced composites, cellular materials, and designed structures, where surface measurements alone may provide incomplete information about the deformation process [45,46]. Zaplatić et al.[45] presented a multimodal experimental approach combining visible-light imaging, infrared thermography, X-ray computed tomography, and Digital Volume Correlation (DVC) for the characterisation of deformation and damage evolution in woven glass fibre composites. Their results demonstrated that volumetric full-field measurements enable detailed analysis of internal strain localisation, shear band formation, and complex damage mechanisms that cannot be fully captured using surface measurements alone. Although DVC introduces greater experimental and computational complexity compared to conventional two-dimensional DIC approaches, it represents an important extension of correlation-based full-field measurement techniques in experimental mechanics.

3.5. Displacement and Strain Computation

The primary output of a digital image correlation analysis is the displacement field describing the motion of points on the specimen surface between a reference and a deformed configuration. For a two-dimensional DIC measurement, the displacement field is typically expressed as:

$$\boldsymbol{u}(x) = \begin{bmatrix} u(x) \\ v(x) \end{bmatrix} \tag{1}$$

where u and v denote the in-plane displacement components along the x and y directions, respectively, and $\mathbf{x}$ = *(x, y)* represents the spatial coordinates in the reference configuration [2]. In local, subset-based DIC, displacement values are obtained at discrete measurement points corresponding to subset centres. The displacement field therefore represents a sampled approximation of the underlying continuous deformation field. Strain fields are not measured directly but are derived from the displacement field through spatial differentiation. This separation between displacement measurement and strain computation is a defining characteristic of most local DIC implementations [2].

For small deformations, strain is commonly computed using the infinitesimal strain tensor, defined as:

$$\boldsymbol{\epsilon} = \frac{1}{2}\left(\boldsymbol{\nabla u} + (\boldsymbol{\nabla u^T})\right) \tag{2}$$

In component form, for a two-dimensional strain tensor, this yields:

$$\epsilon_{xx} = \frac{\partial u}{\partial x},\ \epsilon_{yy} = \frac{\partial v}{\partial y},\ \epsilon_{xy} = \frac{1}{2}\left(\frac{\partial u}{\partial y} + \frac{\partial v}{\partial x}\right) \tag{3}$$

This formulation is widely used in experimental mechanics when deformation remains within the small-strain regime [2]. In cases involving moderate to large deformations or rotations, finite-strain measures are more appropriate. A commonly adopted formulation is the Green–Lagrange strain tensor [47], defined as:

$$\boldsymbol{E} = \frac{1}{2}(\boldsymbol{F}^T\boldsymbol{F} - \boldsymbol{I}) \tag{4}$$

Where:

$$\boldsymbol{F} = \boldsymbol{I} + \nabla \boldsymbol{u} \tag{5}$$

F is the deformation gradient tensor, and **I** denote the identity tensor [2,36]. The choice of strain measure must therefore be consistent with the magnitude of deformation and the intended mechanical interpretation. In practice, spatial derivatives of the displacement field are computed numerically from discrete displacement data. Common approaches include finite-difference schemes [2,33,34,43] and local polynomial fitting [33,34,43] over a defined strain window (i.e. local region over which displacement data are differentiated or fitted to estimate strain). Finite-difference methods offer high spatial resolution but are particularly sensitive to noise, while polynomial fitting approaches provide inherent smoothing at the expense of reduced spatial resolution [29].

Because numerical differentiation amplifies high-frequency noise, strain computation is generally more sensitive to measurement uncertainty than displacement estimation [30]. This sensitivity has been extensively documented in DIC literature and represents a fundamental limitation of local strain computation from discrete displacement data [2,3]. As a result, a trade-off must be established between spatial resolution and noise reduction through appropriate selection of subset size, strain window size, and smoothing or regularisation strategies [30]. Consequently, strain fields obtained from DIC should always be interpreted in the context of the underlying displacement uncertainty and the chosen differentiation methodology [30]. Transparent reporting of strain computation parameters is therefore essential to ensure reliable and reproducible full-field measurements [2,29].

3.6. Accuracy, Uncertainty and Error Sources

The accuracy of digital image correlation measurements is influenced by a combination of experimental, optical, and numerical factors [30]. Key contributors include image noise, speckle pattern quality, subset size, interpolation schemes, camera calibration accuracy, and lighting stability (for example, flickering of LED light sources can introduce significant errors in DIC measurements, and therefore careful selection of illumination equipment is essential) [2,29]. Because DIC relies on tracking grey-level intensity patterns, any factor that degrades image quality or violates the assumed grey-level conservation directly impacts measurement accuracy [30].

Systematic errors may arise from several sources. Lens distortion and imperfect camera calibration introduce spatially varying errors in displacement measurements, particularly in large fields of view or stereo-DIC configurations [2,3,39]. Out-of-plane motion in nominally two-dimensional experiments leads to apparent in-plane displacements due to perspective effects, representing a well-known limitation of 2D-DIC when deformation deviates from planar assumptions [2]. Additionally, violations of the grey-level conservation assumption caused by illumination changes, surface reflections, or temperature-dependent emissivity variations can introduce bias in correlation results [2,30].

Interpolation and subset formulation also contribute significantly to systematic error. The choice of intensity interpolation scheme directly affects sub-pixel displacement accuracy, i.e. the ability of the DIC algorithm to resolve displacements smaller than one pixel by estimating fractional pixel shifts from grayscale intensity variations. If the interpolation scheme does not accurately represent the underlying intensity field, it can introduce measurable bias, meaning a consistent, non-random error where the estimated displacement systematically deviates from the true value, even under ideal conditions [2]. Similarly, when using global DIC approaches mismatches between subset shape functions and the actual deformation field can lead to systematic displacement and strain errors, especially when strong deformation gradients are present [3].

Beyond systematic effects, measurement uncertainty represents an inherent characteristic of DIC results [39]. Experimental and numerical investigations have demonstrated that displacement uncertainty increases with image noise and decreases with increasing subset size, while strain uncertainty is strongly amplified by numerical differentiation of displacement data [29,30]. Consequently, strain measurements are generally more sensitive to noise than displacement measurements, and uncertainty levels depend critically on the selected strain computation strategy and spatial smoothing parameters [3,30].

These findings have led to the recognition that uncertainty quantification is an essential component of modern DIC practice. Best-practice guidelines therefore emphasise rigorous experimental design, careful selection of correlation and differentiation parameters, and transparent reporting of all analysis settings to ensure reliable, repeatable, and comparable full-field measurements [2,29,30].

3.7. Open-source DIC Software and Community Platforms

A diverse ecosystem of open-source digital image correlation software and community-driven platforms has emerged in recent years, reflecting increasing emphasis on transparency, reproducibility, and methodological benchmarking in experimental mechanics. Modular frameworks such as OpenCorr [43] provide extensible environments for the development, testing, and benchmarking of DIC algorithms. OpenCorr is specifically designed for methodological research, allowing users to implement and compare different correlation criteria, shape functions, and optimisation schemes within a unified and transparent framework. High-performance software such as DICe (Digital Image Correlation Engine) [32] focuses on robust and scalable DIC analysis for large datasets. DICe supports both local [2,41] subset-based and global [2,41] finite-element-based correlation strategies within a single software architecture, enabling systematic comparison of different formulations while maintaining computational efficiency.

Widely used subset-based local DIC tools include NCorr [33], which provides a transparent MATLAB implementation suitable for research and educational purposes, and pyDIC [34], a Python-based implementation developed with emphasis on accessibility and reproducibility. Both tools offer full control over correlation parameters and are well suited for experimental studies involving heterogeneous deformation and large strain gradients [33,34].

With respect to global digital image correlation, the number of fully open-source and actively maintained implementations is more limited. A well-established example is Correli [48], a finite-element-based global DIC [2,41] code developed for research applications, in which the displacement field is represented using global shape functions defined over the entire region of interest. Correli has been widely used in studies comparing local and global DIC formulations and remains one of the few openly available global DIC software packages.

In parallel with software development, dedicated community resources and professional society platforms play a critical role in consolidating knowledge and promoting best practices. The Digital Image Correlation Society [49] maintains a central platform providing methodological guidelines, documentation, and links to benchmark datasets. These resources support reproducible research, algorithm comparison, and transparent validation of experimental results across different laboratories and application domains [49].

Table 3.1. Comparison of Digital Image Correlation (DIC) Software in Terms of Implementation and Availability

Software / Platform	Local	Global	Open source	Link
OpenCorr	✓	✓ (framework)	✓	https://opencorr.org/
DICe	✓	✓	✓	https://github.com/dicengine/dice
NCorr	✓	–	✓	https://www.ncorr.com/
pyDIC	✓	–	✓	https://github.com/ladisk/pyDIC
Correli	–	✓	✓	http://www.correlidic.org/
DIC Society	–	–	✓	https://digitalimagecorrelation.org/

3.8. Limitations and Summary

Despite its widespread adoption and versatility, digital image correlation is subject to several inherent limitations that must be carefully considered when designing experiments and interpreting results. First, DIC is an optical technique and therefore requires clear visual access to the specimen surface. Measurement accuracy is strongly dependent on surface preparation, lighting conditions, and image quality, making the technique sensitive to reflections, shadows, and changes in illumination that may violate the grey-level conservation assumption [2,29].

In two-dimensional DIC configurations, accurate measurements further rely on the assumption of negligible out-of-plane motion. When this assumption is violated, apparent in-plane displacements may arise due to perspective effects, leading to systematic measurement errors. Although three-dimensional stereo-DIC systems mitigate this limitation, they introduce additional complexity related to camera calibration, synchronisation, and increased experimental setup requirements [2,38].

From a numerical perspective, strain computation represents a fundamental limitation of local, subset-based DIC. Because strain fields are obtained through spatial differentiation of discrete displacement data, they are inherently more sensitive to image noise and correlation errors. This sensitivity necessitates the use of smoothing, filtering, or regularisation techniques, which in turn introduce a trade-off between spatial resolution and measurement uncertainty [3,29]. Consequently, strain fields should always be interpreted in the context of the chosen differentiation strategy and associated uncertainty.

Global and integrated DIC formulations address some of these limitations by enforcing displacement continuity and incorporating mechanical constraints, thereby improving robustness to image noise. However, these approaches depend strongly on modelling assumptions and may be less suitable for capturing highly localised deformation, displacement discontinuities, or complex material behaviour [36,41]. As a result, no single DIC formulation is universally optimal, and method selection must be guided by experimental objectives, deformation characteristics, and practical constraints.

To summarize, Digital Image Correlation provides a powerful framework for full-field displacement and strain measurement in experimental mechanics, offering capabilities that are difficult or impossible to achieve with traditional point-based techniques. This chapter has reviewed the fundamental principles of DIC, with particular emphasis on local, subset-based formulations, as well as practical considerations related to image acquisition, correlation strategies, displacement and strain computation, accuracy, and uncertainty. The availability of open-source software, benchmark datasets, and community-driven best-practice guidelines has further strengthened the role of DIC as a reliable and reproducible experimental tool.

At the same time, the limitations of DIC—particularly those related to optical access, noise sensitivity, and strain computation—motivate the integration of complementary measurement techniques and advanced data analysis approaches. These considerations provide a natural transition toward the use of Infrared Thermography and artificial intelligence methods.

4. Infrared Thermography (IRT)

While digital image correlation provides detailed full-field information on displacement and strain, mechanical deformation processes are also accompanied by thermal effects that offer complementary insight into material behaviour. Infrared Thermography (IRT) is a non-contact optical measurement technique that enables visualisation of surface temperature fields by detecting thermally emitted radiation. By capturing spatial and temporal temperature variations without interfering with specimen behaviour, thermography has become an important experimental tool for investigating thermomechanical coupling, energy dissipation mechanisms, and damage evolution in materials and structures [6,50].

Unlike contact-based temperature sensors, infrared cameras provide continuous temperature maps over an entire surface, making the technique particularly suitable for experiments involving complex geometries, dynamic loading conditions, and high strain-rate events where conventional instrumentation is difficult to implement. In experimental mechanics, thermography has been widely applied to study deformation-induced heat generation, thermoelastic stress effects, fatigue damage progression, and impact-related energy absorption processes [4,5,7,8,10,11,31,51,52,53].

However, interpretation of thermographic data requires careful consideration of measurement constraints. Temperature estimates are sensitive to emissivity variations, environmental reflections, spatial resolution limitations, and detector noise, all of which may affect accuracy if not properly controlled [6,54]. Furthermore, temperature fields provide indirect indicators of mechanical processes and therefore require coupling with thermomechanical models or integration with complementary full-field measurement techniques [55,56].

4.1. Fundamentals of Infrared Radiation

Infrared Thermography (IRT) is a non-contact optical measurement technique that enables remote mapping of temperature fields by detecting thermally emitted radiation from material surfaces. All bodies with a temperature above absolute zero emit electromagnetic radiation due to thermal motion of charged particles, and the spectral distribution of this radiation depends on temperature and surface properties [6,50,57].

For an ideal blackbody, the total emitted radiation follows the Stefan–Boltzmann law:

$$E = \sigma T^4 \tag{6}$$

where E is radiative exitance, T absolute temperature, and σ the Stefan–Boltzmann constant. Real materials deviate from ideal blackbody behaviour and emit radiation according to their emissivity ε:

$$E = \varepsilon\sigma T^4 \tag{7}$$

Emissivity depends on material composition, oxidation state, surface roughness, coatings, and viewing angle. In experimental mechanics applications, incorrect emissivity estimation is one of the primary sources of systematic temperature measurement error [6,50].
It is important to distinguish temperature from heat. Temperature describes a thermodynamic state variable associated with particle motion, whereas heat represents energy transfer due to temperature differences. Infrared thermography therefore measures surface temperature distributions rather than heat flux directly, and mechanical interpretation requires coupling with thermomechanical models [57].

4.2. Infrared Cameras and Measurement Principles

Infrared cameras measure surface temperature by detecting the thermal radiation emitted by an observed object within specific wavelength bands of the infrared spectrum. In most thermographic systems used in experimental mechanics, measurements are performed in either the mid-wave infrared (MWIR, 3–5 µm) or long-wave infrared (LWIR, 8–14 µm) spectral regions (see Figure 4.1.). These wavelength ranges correspond to the peak radiation emitted by objects at typical engineering temperatures and therefore allow efficient temperature measurement without external illumination [50,58].

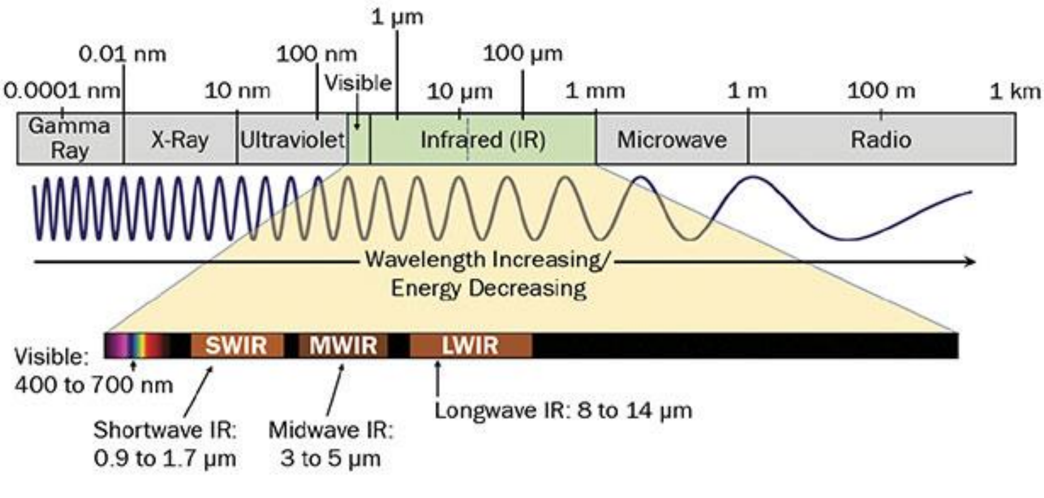

Figure 4.1. Overview of the electromagnetic spectrum with emphasis on the infrared region, showing wavelength ranges of shortwave (SWIR), midwave (MWIR), and longwave (LWIR) infrared radiation relevant for thermographic measurements[59].

The radiation emitted by a surface is collected through an infrared-transparent optical system and focused onto a detector array. Modern infrared cameras typically employ microbolometer detectors for uncooled LWIR cameras or photon detectors in cooled MWIR systems. Microbolometers measure temperature-induced changes in electrical resistance caused by absorbed radiation, while photon detectors convert incoming infrared photons directly into electrical signals. Cooled photon detectors generally provide higher sensitivity and faster response times, whereas uncooled microbolometers offer lower cost and simpler operation [58,60,61].

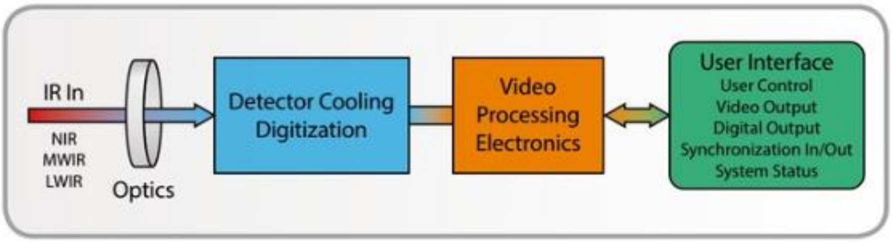

Figure 4.2. Simplified diagram of an infrared camera showing optics, detector array, and signal processing stages [62].

The electrical signal generated by the detector is processed through calibration algorithms that convert measured radiation intensity into temperature values (see Figure 4.2.). This conversion requires knowledge of several parameters, including object emissivity, reflected environmental radiation, and atmospheric transmission between the object and the camera. Accurate thermographic measurements therefore depend not only on detector performance but also on proper experimental setup and calibration procedures [6,54].

Several camera characteristics influence the quality of thermographic measurements in mechanical experiments. One of the most important parameters is the Noise Equivalent Temperature Difference (NETD, see Figure 4.3.), which represents the smallest temperature variation that can be distinguished from detector noise. Lower NETD values correspond to higher thermal sensitivity and allow detection of weak thermal signals generated during for example elastic deformation stages [58].

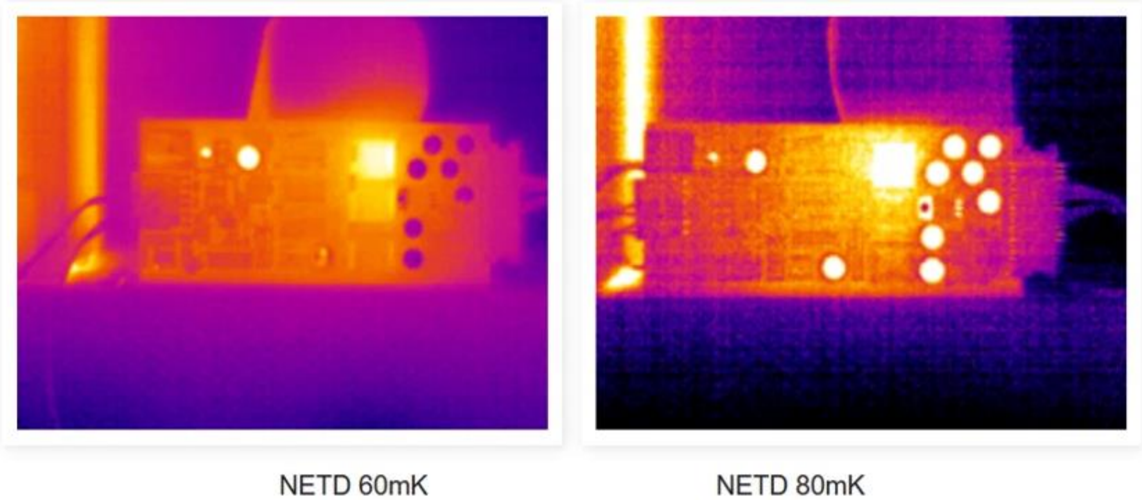

Figure 4.3. Example illustrating temperature resolution limits determined by detector noise [63].

Another important factor is spatial resolution, which depends on the detector pixel size, optical magnification, and distance between the camera and the specimen. Limited spatial resolution may reduce the ability to detect small thermal features or highly localised deformation zones.

In addition, frame rate and integration time determine the temporal resolution of the measurement. High frame rates are necessary to capture transient thermal events in dynamic experiments, but increasing acquisition speed typically reduces signal-to-noise ratio and temperature accuracy [8,61].

Because thermographic measurements rely on radiation rather than direct temperature sensing, environmental conditions such as reflections from surrounding surfaces and variations in emissivity can introduce systematic errors. Careful experimental design, calibration, and surface preparation are therefore required to ensure reliable temperature measurements during mechanical testing [54].

4.3. Passive and Active Thermography

Infrared Thermography techniques are commonly classified into passive and active approaches depending on whether the observed temperature variations arise naturally or are induced through external thermal excitation. This distinction is important when selecting an appropriate thermographic method for a particular experimental application [6,52].

4.3.1. Passive Thermography

Passive thermography relies on naturally occurring temperature variations generated by physical processes within the observed system. In mechanical testing, these temperature changes arise from thermomechanical phenomena such as elastic deformation, plastic dissipation, friction, and damage evolution. Because no external heat source is required, passive thermography allows observation of temperature fields without influencing the mechanical behaviour of the specimen [8]. In experimental mechanics, passive thermography is particularly valuable for analysing energy dissipation mechanisms during deformation. As materials undergo plastic deformation (see Figure 4.4.), a large fraction of the mechanical work is converted into heat, producing local temperature rises that can be detected by infrared cameras. This behaviour can be described through the Taylor–Quinney relation, which links plastic deformation work to thermal energy generation. Consequently, thermographic measurements provide spatially resolved information about the distribution of dissipated mechanical energy within the material [64,65].

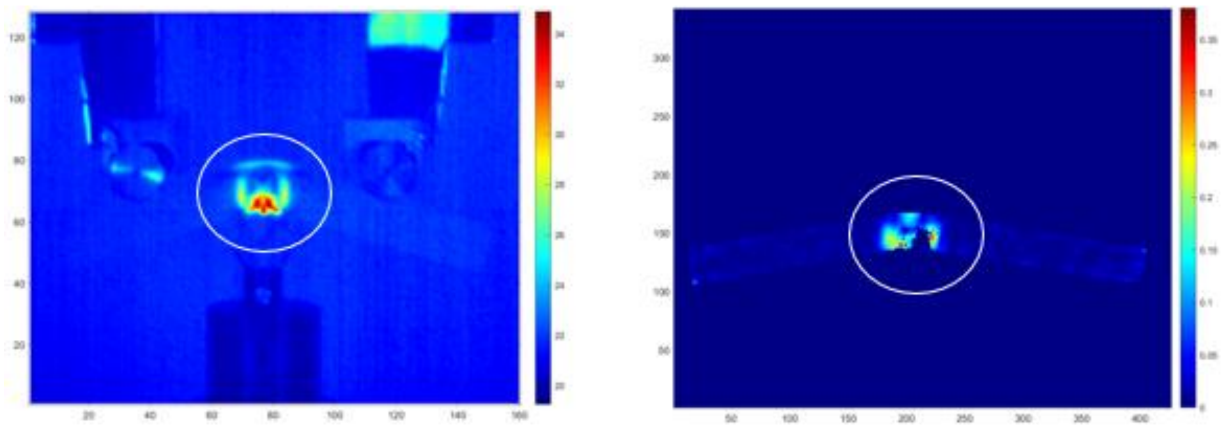

Figure 4.4. Infrared Thermography (left) and Digital Image Correlation (right) associated image showing temperature increase associated with plastic deformation during mechanical loading.

In addition to plastic dissipation, passive thermography can also detect thermoelastic temperature changes occurring during purely elastic deformation. Under adiabatic conditions, tensile stresses typically produce small temperature decreases, while compressive stresses produce slight temperature increases. Although these thermoelastic signals are generally small in magnitude, they provide useful information about stress distributions and can be exploited in thermoelastic stress analysis techniques [4,51].

4.3.2. Active Thermography

In contrast to passive thermography, active thermography involves deliberately applying an external thermal stimulus to the specimen in order to generate a measurable temperature response (see Figure 4.5.). Common excitation methods include short heat pulses, periodic heating, or optical stimulation using high-power lamps or lasers. The resulting transient temperature field is analysed to identify subsurface defects, material inhomogeneities, or structural damage [52,66].
Active thermography techniques are widely used in non-destructive evaluation (NDE) and structural inspection. Methods such as pulse thermography and lock-in thermography enhance the detection of internal defects by observing differences in heat diffusion behaviour within the material. Regions containing voids, cracks, or inclusions alter the propagation of thermal waves, producing detectable temperature contrasts on the surface [52].

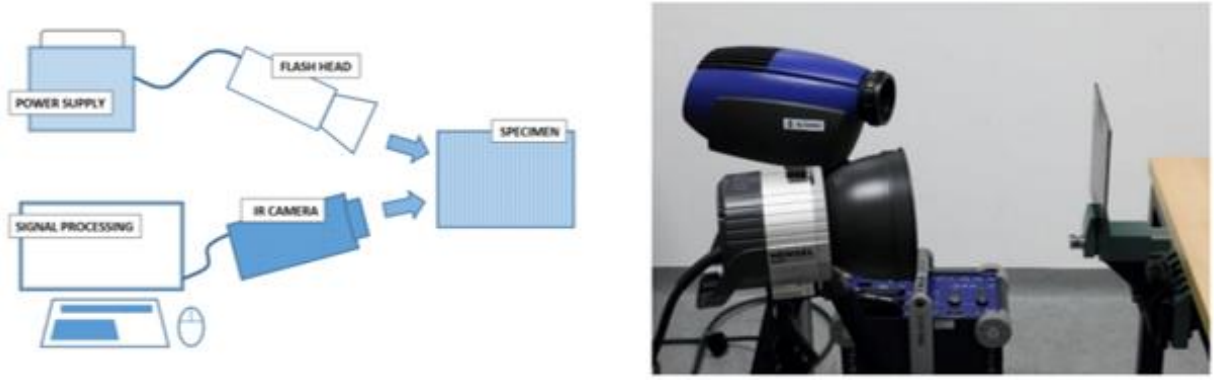

Figure 4.5. Example of Pulse Phase Thermography [67].

Despite their usefulness in inspection applications, active thermography techniques are generally less suitable for mechanical testing experiments. External heating may alter the thermal boundary conditions of the specimen, potentially influencing the deformation process or masking thermomechanical temperature changes associated with mechanical loading. In addition, mechanical testing setups often involve loading frames, fixtures, or protective enclosures that complicate the application of controlled thermal excitation.

For these reasons, passive thermography is typically preferred in experimental mechanics, where the objective is to observe temperature changes directly associated with deformation processes. By capturing temperature fields generated by thermomechanical coupling and plastic dissipation, passive thermography provides valuable insight into material behaviour without interfering with the mechanical experiment.

4.4. Thermomechanical Coupling and Heat Generation

Mechanical deformation of materials is inherently coupled with thermal effects, as part of the applied mechanical work is either stored within the material or dissipated in the form of heat. This coupling plays an important role in experimental mechanics, where temperature measurements obtained through infrared thermography provide indirect information about deformation processes. From a thermodynamic perspective, the total mechanical work can be partitioned into recoverable elastic energy and irreversible dissipative components, the latter being associated with heat generation [8,56].

4.4.1. Thermoelastic Effect (Elastic Regime)

During elastic deformation, materials exhibit small and reversible temperature changes associated with the thermoelastic effect. Under adiabatic conditions, variations in hydrostatic stress produce corresponding temperature changes, which can be expressed in simplified form as:

$$\Delta T = -\frac{T}{\rho c}\,\Delta\sigma_h \tag{8}$$

where ΔT is the temperature change, T the absolute temperature, ρ the material density, c the specific heat capacity, and $\Delta\sigma$ change in hydrostatic stress [4,51].
In practical terms, tensile loading results in a slight temperature decrease, while compressive loading produces a small temperature increase. These temperature variations are reversible and

typically of very low magnitude, often requiring high-sensitivity infrared systems for detection. Despite their small amplitude, thermoelastic effects provide useful information about stress distributions and form the basis of thermoelastic stress analysis methods [4].

4.4.2. Heat Generation during Plastic Deformation

When the material response transitions from elastic to plastic behaviour, the thermomechanical response becomes dominated by irreversible processes. Plastic deformation involves mechanisms such as dislocation motion, microstructural rearrangements, and internal friction, all of which contribute to energy dissipation in the form of heat. As a result, measurable temperature increases develop in regions undergoing plastic deformation [8,65]. The relationship between plastic work and heat generation is commonly described using the Taylor–Quinney framework:

$$\Delta Q = \beta \, \Delta W_p \tag{9}$$

where ΔW_p represents the plastic deformation work, ΔQ the generated heat, and β the fraction of plastic work converted into thermal energy [8,56,64,65].

For ductile materials, including aluminium alloys, a large portion of plastic work is dissipated as heat, particularly under conditions of moderate to high strain rates. Experimental investigations have shown that this conversion becomes increasingly efficient under near-adiabatic conditions, where limited heat diffusion leads to localised temperature rise [56,65]. Consequently, local temperature increases observed using Infrared Thermography can be directly associated with zones of high energy dissipation within the material (see Figure 4.6.) [8,65].

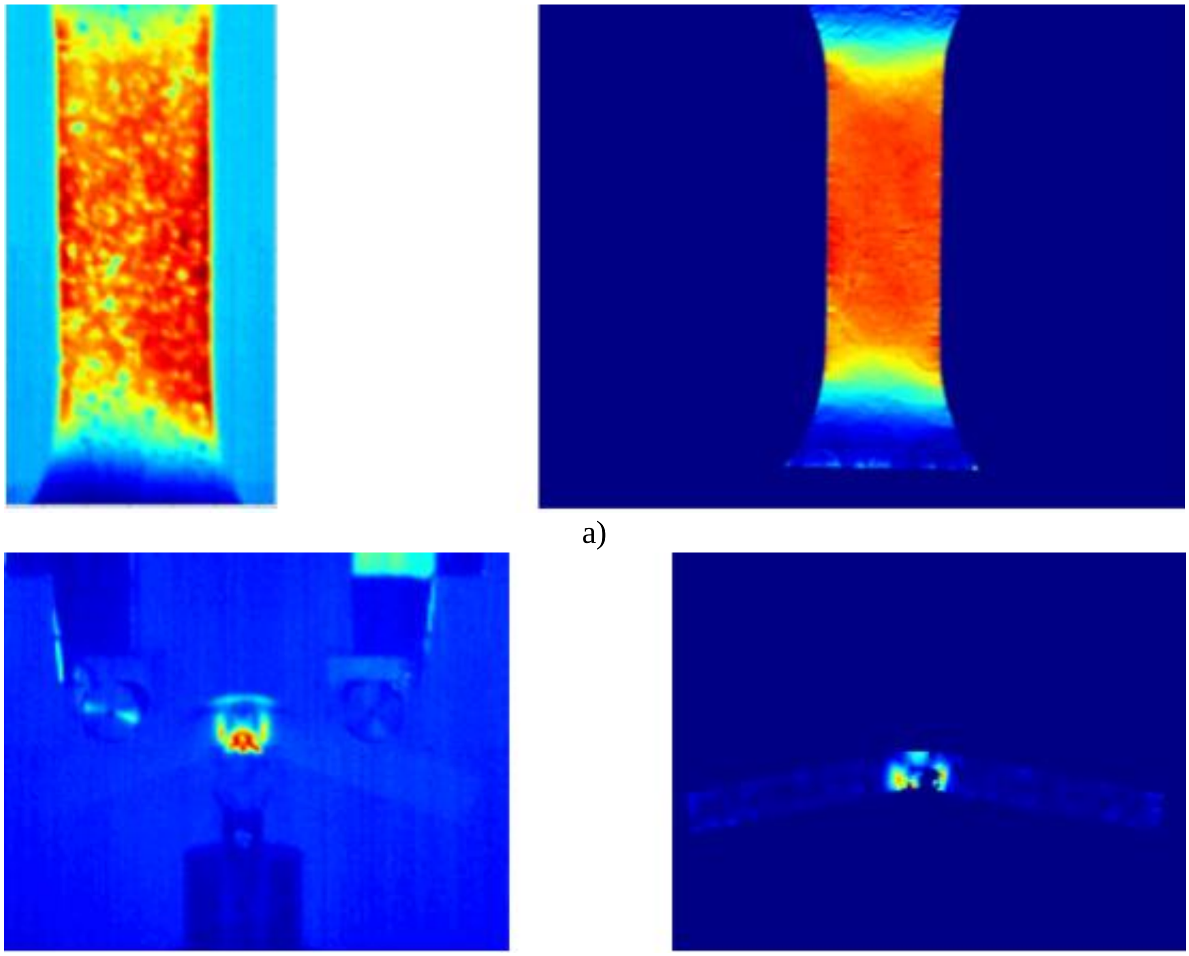

a)

b)

Figure 4.6. Thermographic response during mechanical loading: a) full-field temperature distribution illustrating global heat generation in relation to Effective strain for dog bone specimen; b) localised thermal response highlighting zones of deformation and energy dissipation for three-point bending specimen.

The temperature increase associated with plastic deformation is therefore closely related to the local rate of energy dissipation. In materials exhibiting heterogeneous deformation behaviour, such as cellular or auxetic structures, deformation is often highly localised. This results in concentrated heat generation that appears as localised hotspots in thermographic images, enabling identification of regions with elevated plastic strain and energy absorption [8,65].

4.4.3. Combined Thermomechanical Response

In practical experiments, the measured temperature field is typically a combination of both thermoelastic and dissipative contributions. At low stress levels, thermoelastic effects dominate and temperature variations remain small and reversible, while plastic dissipation remains negligible [4,51]. As loading increases and plastic deformation develops, irreversible heat generation progressively becomes the dominant mechanism governing the thermal response [8].

The relative contribution of these effects depends on material properties, strain rate, and boundary conditions. In high strain-rate or impact loading, deformation often occurs under near-adiabatic conditions, meaning that heat generated during plastic deformation remains localised and closely reflects the distribution of mechanical work [8,65]. In contrast, during quasi-static loading, heat conduction may redistribute thermal energy, reducing the apparent temperature rise and limiting quantitative interpretation of thermographic data [8,65].

4.4.4. Implications for Experimental Mechanics

The coupling between mechanical deformation and thermal response provides a strong physical basis for the application of infrared thermography in experimental mechanics. Since temperature changes are directly related to energy dissipation, thermographic measurements can be interpreted as spatial representations of deformation energy, particularly in regimes dominated by plasticity [8,65]. However, temperature fields represent indirect measurements of mechanical behaviour and must be interpreted with care. Factors such as heat conduction, emissivity variations, environmental reflections, and experimental conditions can influence the measured temperature distribution [6,66]. For this reason, thermography is often combined with full-field displacement measurement techniques, such as Digital Image Correlation, to provide a more complete description of deformation processes by linking mechanical fields with energy dissipation mechanisms (see Figure 4.6.) [65].

4.5. Applications in Experimental Mechanics

Infrared Thermography has become an established tool in experimental mechanics for analysing deformation processes, damage evolution, and energy dissipation in materials and structures. Its ability to provide non-contact, full-field temperature measurements makes it particularly suitable for studying complex mechanical behaviour under a wide range of loading conditions, including quasi-static, cyclic, and dynamic regimes [8,65].

One of the primary applications of infrared thermography in experimental mechanics is the investigation of plastic deformation and energy dissipation. As discussed in previous sections, plastic work is largely converted into heat, enabling thermographic measurements to reveal zones of high energy absorption. This has been widely applied in studies of metals, polymers, and composite materials, where temperature fields are used to identify strain localisation, necking, and the onset of plasticity [8,56,65].

Infrared Thermography is also extensively used in the analysis of fatigue and damage evolution. During cyclic loading, temperature changes can be associated with energy dissipation mechanisms such as microplasticity and crack initiation. Thermographic techniques have been successfully employed to detect early-stage damage and to estimate fatigue limits based on thermal signatures, offering a non-destructive alternative to conventional fatigue testing methods [8,68,69].

In addition to quasi-static and cyclic loading, thermography has proven particularly valuable in high strain-rate and impact experiments, where rapid deformation leads to significant heat generation. Under such conditions, deformation often occurs in a near-adiabatic regime, and temperature fields closely reflect the spatial distribution of plastic work. Thermographic measurements in impact tests have been used to study strain localisation, energy absorption mechanisms, and failure processes in structural materials [65].

Infrared Thermography is also increasingly applied to the study of custom-designed structures and cellular materials, including auxetic structures and metamaterials. These materials exhibit complex deformation mechanisms such as bending, buckling, and rotation of structural elements, leading to highly heterogeneous energy dissipation patterns. Thermographic measurements enable direct visualisation of these processes by highlighting regions of concentrated heat generation, providing insight into deformation mechanisms that are difficult to capture using conventional measurement techniques [8].

Another important application is the use of thermography in thermoelastic stress analysis (TSA), where small temperature variations associated with elastic deformation are used to infer stress distributions. Although the thermoelastic effect produces relatively small temperature changes, advances in infrared camera sensitivity have enabled its application in stress analysis of engineering components, particularly under cyclic loading conditions [4,51].

More recently, Infrared Thermography has been combined with other full-field measurement techniques, such as Digital Image Correlation, to provide a comprehensive description of material behaviour. This combined approach enables simultaneous measurement of displacement, strain, and temperature fields, allowing direct correlation between mechanical deformation and energy dissipation. Such multimodal experimental frameworks are increasingly used in advanced materials research and provide a foundation for data-driven and machine learning approaches in experimental mechanics [5,8,15,16].

4.6. Limitations and Summary

Despite its versatility and non-contact nature, Infrared Thermography presents several limitations that must be considered when interpreting experimental results.
From a measurement perspective, temperature estimation depends strongly on surface emissivity, environmental reflections, and calibration accuracy. Variations in emissivity or uncontrolled reflections may introduce systematic errors, particularly when dealing with heterogeneous materials or changing surface conditions [6,54].
Thermography also provides an indirect measurement of mechanical behaviour, as temperature fields represent the thermal response rather than the deformation itself. The interpretation of thermographic data therefore requires careful consideration of thermomechanical coupling, particularly when distinguishing between thermoelastic and dissipative effects [8,65]. In addition, heat conduction may redistribute thermal energy over time, reducing spatial resolution and complicating quantitative analysis, especially under quasi-static loading conditions [8,65].

Experimental constraints further affect measurement quality. Infrared cameras typically exhibit a trade-off between spatial resolution, temporal resolution, and thermal sensitivity, which may limit their applicability in high-speed or small-scale experiments. In dynamic testing scenarios, additional challenges may arise from experimental setups, such as protective enclosures or impact shielding, which can be opaque to infrared radiation and prevent direct temperature measurement of the region of interest.
Finally, the quantitative interpretation of thermographic data remains sensitive to noise, boundary conditions, and modelling assumptions. While temperature fields can be directly related to energy dissipation under near-adiabatic conditions, this relationship becomes less straightforward when heat transfer effects are significant or when material behaviour deviates from idealised assumptions [8,56].
Despite these limitations, Infrared Thermography remains a powerful tool in experimental mechanics, particularly when combined with complementary full-field measurement techniques and supported by careful experimental design and data interpretation.

5. Artificial Intelligence in Experimental Mechanics

The increasing availability of high-resolution experimental data has significantly influenced the development of modern experimental mechanics. Techniques such as Digital Image Correlation and Infrared Thermography generate dense full-field measurements of displacement, strain, and temperature, enabling detailed analysis of complex material behaviour. However, the volume and complexity of such data often exceed the capabilities of traditional analysis methods, particularly when dealing with heterogeneous deformation, noise, and coupled physical phenomena.

Artificial intelligence (AI), and in particular machine learning, provides a framework for extracting meaningful information from such data by learning relationships directly from measurements. Unlike classical approaches based solely on physical modelling, AI methods enable the identification of patterns, correlations, and mappings that may not be readily accessible through analytical formulations. This is especially relevant in experimental mechanics, where inverse problems, data fusion, and high-dimensional datasets are common [13,14].

Recent advances in deep learning have further accelerated the integration of AI into experimental workflows. Deep neural networks are capable of processing image-based data directly, making them well suited for applications involving full-field measurements. In this context, displacement fields, strain maps, and thermal images can be interpreted as structured data, allowing the application of computer vision techniques to problems in mechanics [14,70].

Applications of AI in experimental mechanics include full-field data reconstruction, noise reduction, surrogate modelling, and image-to-image translation between different measurement modalities. In particular, the combination of Digital Image Correlation and Infrared Thermography through data-driven models has emerged as a promising approach for linking mechanical deformation with energy dissipation mechanisms. Recent studies have demonstrated the feasibility of predicting thermal fields directly from strain measurements using deep learning models, highlighting the potential of AI-based data fusion frameworks in experimental analysis (see Figure 5.1.) [15,16].

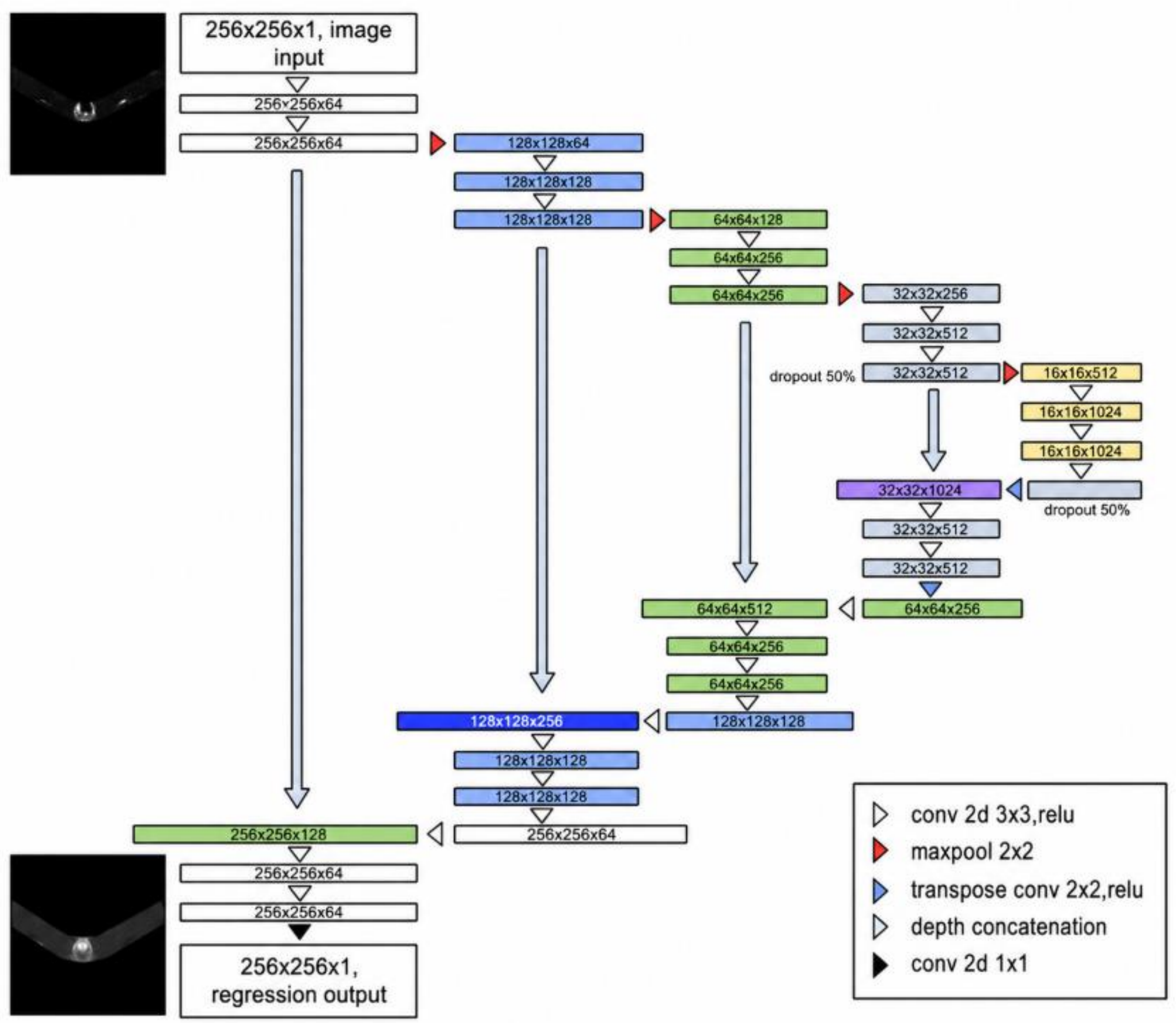

Figure 5.1. Example of integration of experimental measurements (DIC, IRT) with AI-based model (U-Net) for thermal prediction [15].

5.1. Machine Learning and Deep Learning Review

Machine learning (ML) refers to a class of computational methods that enable models to learn relationships between input and output data through experience rather than explicit programming. In contrast to traditional deterministic modelling approaches, ML methods rely on statistical learning principles to approximate complex mappings, making them particularly suitable for systems where governing equations are difficult to formulate or solve [13].

In experimental mechanics, machine learning provides a powerful tool for analysing high-dimensional datasets generated by full-field measurement techniques. These datasets often exhibit spatial correlations, noise, and nonlinear behaviour, all of which can be effectively handled using data-driven approaches. By learning directly from experimental data, ML models can be used for regression, classification, and pattern recognition tasks, such as predicting strain fields, identifying damage, or filtering measurement noise [14].

Machine learning methods are commonly divided into three categories: supervised, unsupervised, and semi-supervised learning. In supervised learning, models are trained using labelled datasets, where both input and corresponding output are known. This approach is widely used in experimental mechanics for tasks such as displacement or temperature field prediction [18,24,71,72,73]. Unsupervised learning aims to identify hidden structures or patterns in data without predefined labels, while semi-supervised learning combines both approaches to leverage limited labelled data [13].

5.1.1. Deep Learning Paradigm

Deep learning represents a subset of machine learning based on artificial neural networks with multiple layers, enabling hierarchical representation learning. Unlike traditional approaches that rely on manually engineered features, deep learning models automatically extract relevant features from raw data during the training process (see Figure 5.2.). This capability is particularly advantageous for image-based datasets, where important information is encoded in spatial structures and patterns [13,14].

In the context of experimental mechanics, deep learning allows direct processing of full-field measurements such as displacement maps or thermal images. These data can be interpreted as images, enabling the use of convolutional neural networks and related architectures to capture spatial dependencies and complex nonlinear relationships (see Figure 5.3.). As a result, deep learning models are capable of identifying deformation patterns, localisation phenomena, and correlations between different physical fields [17,21,22,24,74].

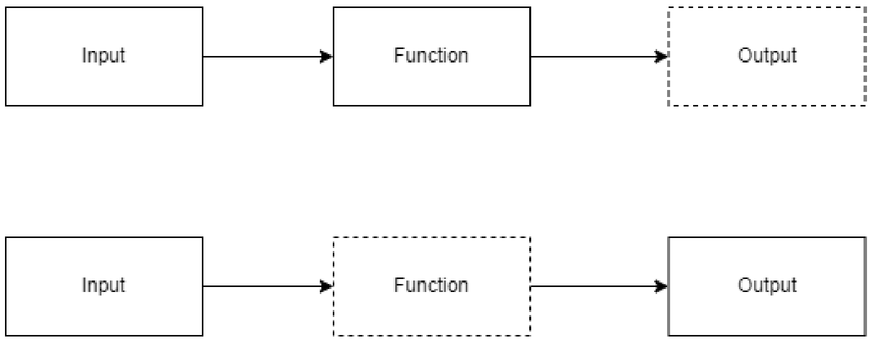

Figure 5.2. Deep learning paradigm

Deep neural networks are typically trained using large datasets and optimised through gradient-based learning algorithms. While this enables high predictive performance, it also introduces challenges related to data dependency, generalisation, and interpretability. These aspects are particularly important in engineering applications, where models must remain robust and physically meaningful under varying experimental conditions [20].

In addition, the transferability of learned features across different datasets and experimental setups remains an important consideration. Studies have shown that while lower-level features learned by neural networks are often transferable, higher-level representations especially under quasi-static loading conditions tend to be more task-specific, which may limit model generalisation when applied to new experimental conditions [75].

5.1.2. Relevance to Experimental Mechanics

The integration of machine learning into experimental mechanics is driven by the need to analyse increasingly complex datasets and to establish relationships between different physical quantities. In particular, deep learning enables the development of models capable of mapping between full-field measurements, such as predicting thermal responses from strain data or enhancing measurement accuracy through data-driven filtering [15,16,17,24,26,27,76].

These capabilities open new possibilities for experimental analysis, including the development of surrogate models, real-time data interpretation, and multimodal data fusion. By combining experimental measurements with AI-based models, it becomes possible to extend the capabilities of traditional measurement techniques and to gain deeper insight into complex deformation and energy dissipation processes [26,27,76].

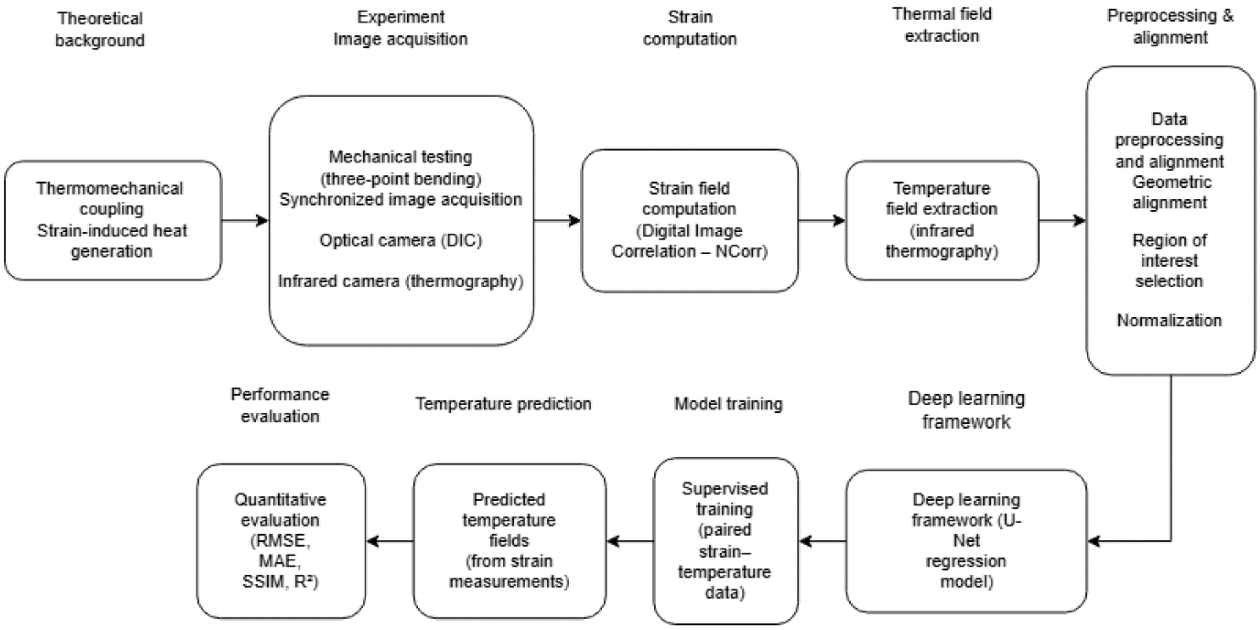

Figure 5.3. Workflow illustrating machine learning applied to full-field experimental data [15].

5.2. Convolutional Neural Networks

Convolutional Neural Networks (CNNs) represent a class of deep learning architectures specifically designed for processing structured data with spatial correlations, such as images. Their development has been largely motivated by computer vision applications, but their ability to learn spatially distributed features makes them particularly suitable for analysing full-field experimental data, including displacement, strain, and temperature fields obtained through techniques such as Digital Image Correlation and Infrared Thermography [14,70].

Unlike traditional fully connected neural networks [13], CNNs exploit the spatial structure of input data through local connectivity and parameter sharing [13,14]. This enables efficient learning of spatial features while significantly reducing the number of trainable parameters, making CNNs both computationally efficient and robust to variations in input data [13,14].

This example highlights the efficiency of convolutional neural networks compared to fully connected architectures (see Figure 5.4.). While fully connected networks require a large number of parameters when applied to image-based data, convolutional layers achieve similar feature extraction capabilities with significantly fewer parameters due to weight sharing and local connectivity [13,14].

Consider an input image (or full-field data) of input size 128 × 128 × 1 representing an image with a single channel, i.e., a grayscale image, thermal image, or effective strain image. If the input is flattened, this gives:

$$128 \times 128 = 16384 \text{ inputs} \tag{10}$$

Assuming we have one hidden layer with 100 neurons:

$$16384 \times 100 = 1638400 \tag{11}$$

With the addition of the bias parameter b = 100, the total number of learned parameters for a single hidden layer is approximately 1.64 million.

Now let’s consider one convolutional layer with 32 filters and a kernel size of 3x3.

Each filter:

$$3\text{x}3\text{x}1 = 9 \text{ weights} \tag{12}$$

With 32 filters:

$$9\text{x}32 = 288 \tag{13}$$

With addition of bias parameter b=32, total number of parameters is 320. This results in a reduction factor of approximately 5000.

In convolutional neural networks, the learning process focuses on estimating a small set of convolutional kernels that are spatially shared across the input. This contrasts with fully connected architectures, where unique weights are learned for each individual input–output connection. As a result, CNNs significantly reduce the number of trainable parameters while preserving spatial structure in the data [13,14].

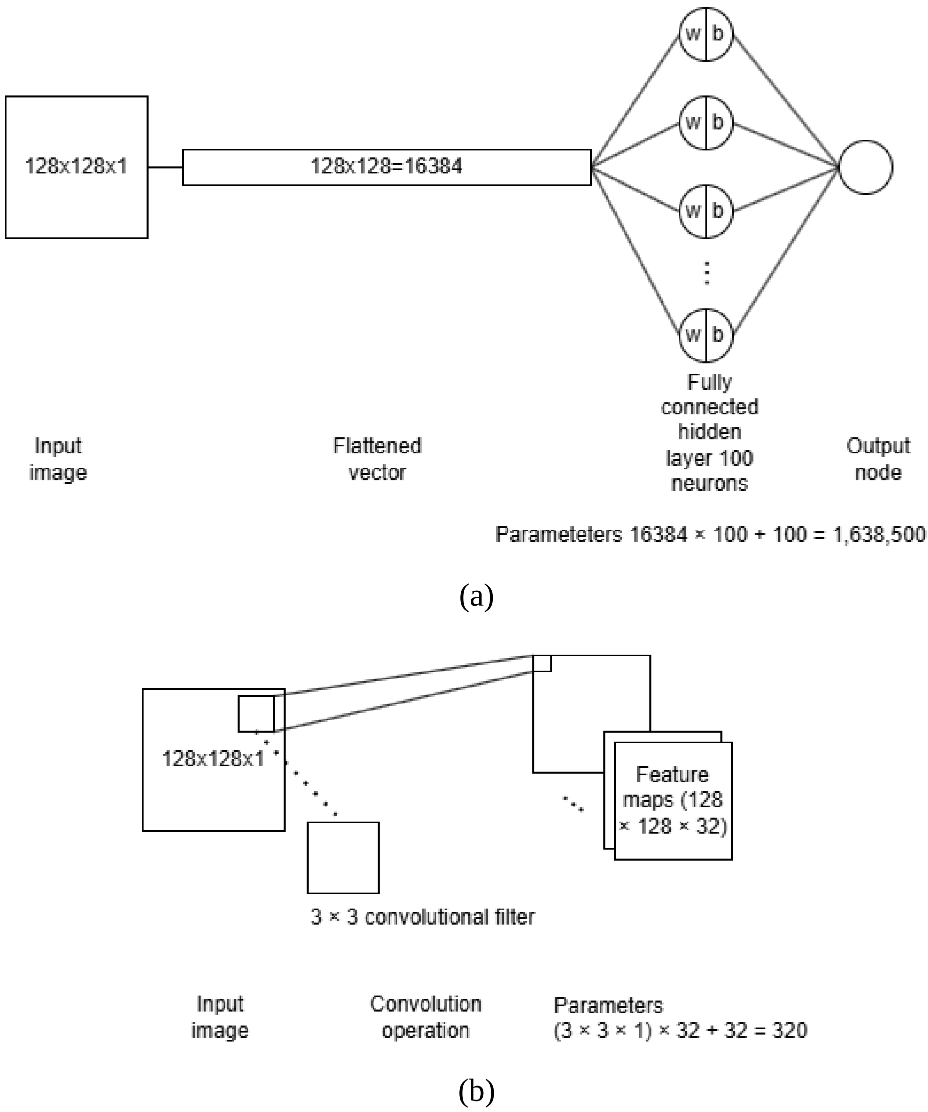

Figure 5.4. Comparison of a) fully connected neural network and b) Convolutional neural network.

5.2.1. Convolutional Operations

The fundamental building block of a CNN is the convolutional layer, which applies a set of learnable filters (kernels) to the input data. Each filter is convolved with the input image to produce a feature map that highlights specific spatial patterns. Mathematically, the convolution operation for a 2D input can be expressed as:

$$y(i,j) = \sum_{m}\sum_{n} x(i+m, j+n)\ w(m,n) + b \tag{14}$$

where *x(i,j)* represents the input image, *w(m,n)* the convolution kernel, *b* a bias term, and *y(i,j)* the resulting feature map[13,14].

This operation enables the detection of local features such as edges, gradients, and textures in early layers, while deeper layers capture more complex and abstract patterns. The use of shared weights ensures that the same feature detector is applied across the entire image, providing translation invariance and improving generalisation [14,77].

Following convolution, nonlinear activation functions (such as ReLU) are applied to introduce nonlinearity into the model, allowing the network to approximate complex mappings[13,14]. Pooling operations may also be used to reduce spatial resolution while retaining the most relevant features, improving robustness to noise and small spatial variations [13].
In experimental mechanics applications, convolutional operations allow CNNs to directly process full-field measurement data. For example, strain localisation patterns, crack initiation zones, and thermal hotspots can be interpreted as spatial features that are automatically extracted by convolutional filters during training.

5.2.2. Feature Extraction and Hierarchical Representations

One of the key strengths of CNNs lies in their ability to learn hierarchical feature representations. Early layers of the network typically capture low-level features such as edges, intensity gradients, and simple textures. Intermediate layers combine these features into more complex structures, while deeper layers encode high-level representations corresponding to physically meaningful patterns such as deformation localisation or damage regions (see Figure 5.5.) [75,77,78].
This hierarchical learning process enables CNNs to replace manual feature engineering, which is often challenging in experimental mechanics due to the complexity and variability of deformation behaviour. Instead of defining features explicitly, the network learns task-specific representations directly from data, allowing it to adapt to for example different materials, loading conditions, and measurement modalities [13,14].

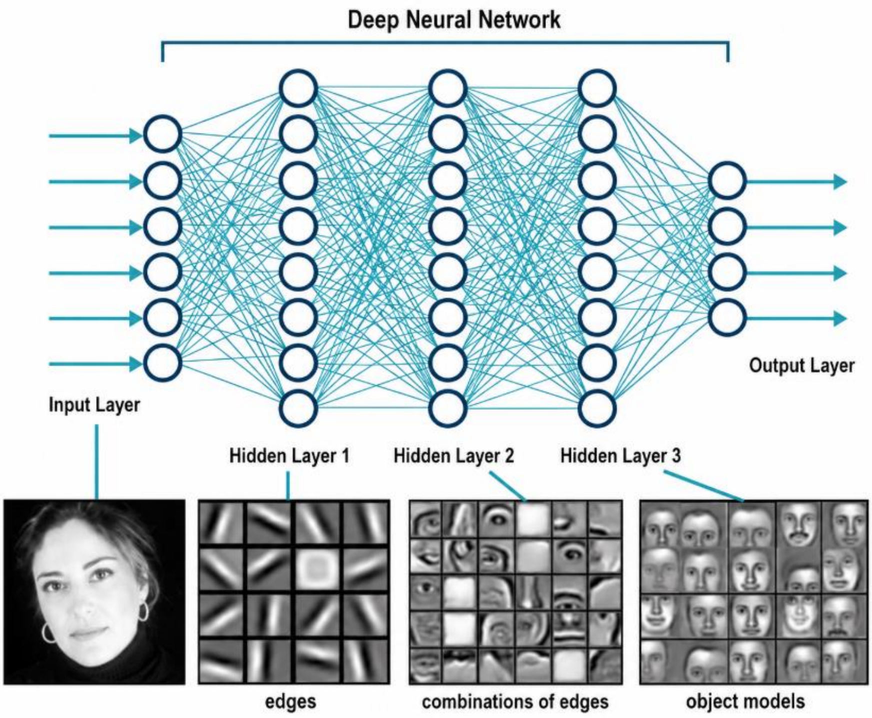

Figure 5.5. Hierarchical feature extraction in a convolutional neural network, illustrating the progression from low-level features (edges and intensity gradients), through mid-level... features (textures and patterns), to high-level representations capturing structural and semantic information [79].

Studies on feature visualisation and transfer learning have shown that lower-level features learned by CNNs are generally transferable across different tasks, while higher-level features become increasingly specialised. This property is particularly relevant in experimental mechanics, where models trained on one dataset may need to be adapted to different experimental conditions or materials [15,75].

Furthermore, CNN-based feature extraction has been successfully applied to full-field experimental data for tasks such as displacement estimation, strain field reconstruction, and defect detection. In these applications, learned features correspond to physically meaningful patterns in the data, enabling improved interpretation and analysis of experimental results [17,21,22].

5.2.3. Relevance to Full-Field Experimental Data

The suitability of CNNs for experimental mechanics arises from the structural similarity between image data and full-field measurements. Displacement fields, strain maps, and thermal images can all be represented as two-dimensional grids, where spatial relationships carry important physical meaning. Convolutional operations preserve these relationships, allowing CNNs to capture correlations between neighbouring points and to identify localised phenomena such as strain concentration or heat generation [13,14,15,17,35].
This makes CNNs particularly effective for:

- image-to-image regression tasks, where one physical field is predicted from another
- noise reduction and data enhancement, improving measurement quality
- feature detection, such as identifying damage or localisation zone

These capabilities form the basis for more advanced architectures, such as encoder–decoder networks [70,80], which are specifically designed for full-field prediction tasks and are discussed in the following section.

5.3. Encoder–Decoder Architectures

Encoder–decoder architectures represent a class of neural network models designed to map input data to structured outputs through an intermediate latent representation (see Figure 5.6.). These models consist of two primary components: an encoder, which compresses the input into a lower-dimensional feature space, and a decoder, which reconstructs the desired output from this representation. The conceptual basis of such architectures originates from autoencoder frameworks, where data compression and reconstruction are jointly optimised [81].

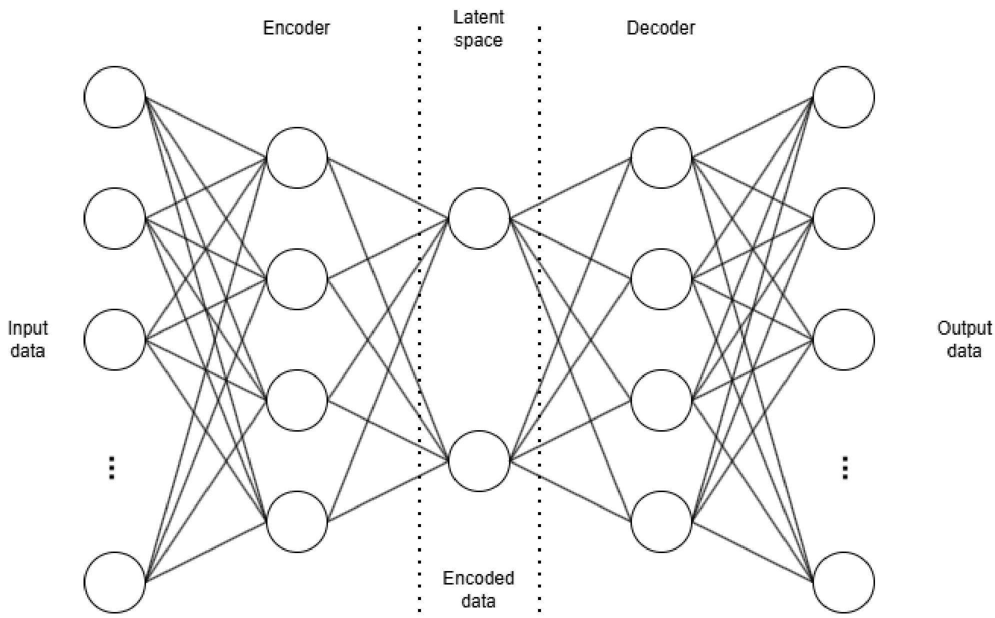

Figure 5.6. Illustration of Encoder-Decoder networks.

The extension of encoder–decoder concepts to convolutional neural networks has enabled their application to image-based and spatially distributed data. In fully convolutional networks, traditional fully connected layers are replaced with convolutional operations, allowing the network to produce dense, pixel-wise predictions while preserving spatial information[80]. This property is essential for applications involving full-field data, where the spatial arrangement of measurements carries physical meaning.

In practical implementations, the encoder progressively reduces the spatial resolution of the input through a series of convolutional and down sampling operations, extracting increasingly abstract feature representations (see Figure 5.7.). This process allows the network to capture both local patterns and global contextual information. The compressed latent representation serves as a compact encoding of the input, containing the most relevant features required for reconstruction or prediction. The decoder then performs the inverse operation, progressively restoring spatial resolution through up sampling or transposed convolution layers, ultimately producing an output with the same or similar dimensions as the input [13,70,80].

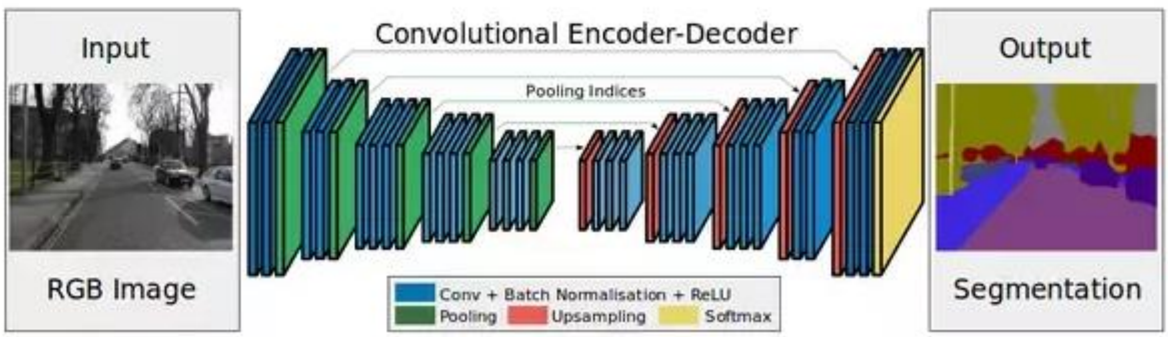

Figure 5.7. Convolutional Encoder-Decoder[82].

A key limitation of early encoder–decoder models is the loss of fine spatial details during the encoding process (see Figure 5.8.) [82].

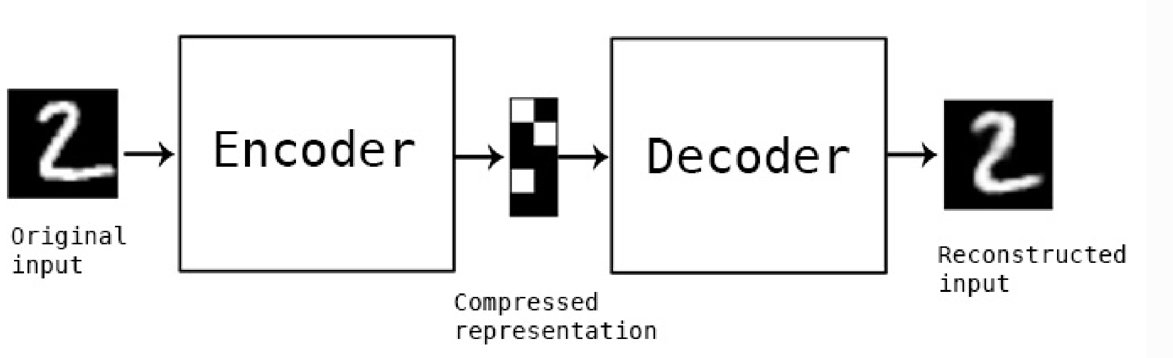

Figure 5.8. Illustration of limitations in encoder-decoder models [83].

This issue was addressed by the introduction of skip connections, most notably in the U-Net architecture, which directly link corresponding layers in the encoder and decoder [70]. These connections allow high-resolution features from early layers to be combined with deeper representations, significantly improving the reconstruction of localised features and sharp boundaries[13,70]. Such properties are particularly important in experimental mechanics, where phenomena such as strain localisation and damage initiation occur at small spatial scales.

Encoder–decoder architectures are especially well suited for image-to-image regression tasks, where the objective is to predict one spatial field from another. This paradigm has been further generalised through conditional generative models, such as pix2pix (see Figure 5.9.), which learns mappings between paired image domains using supervised learning [74].

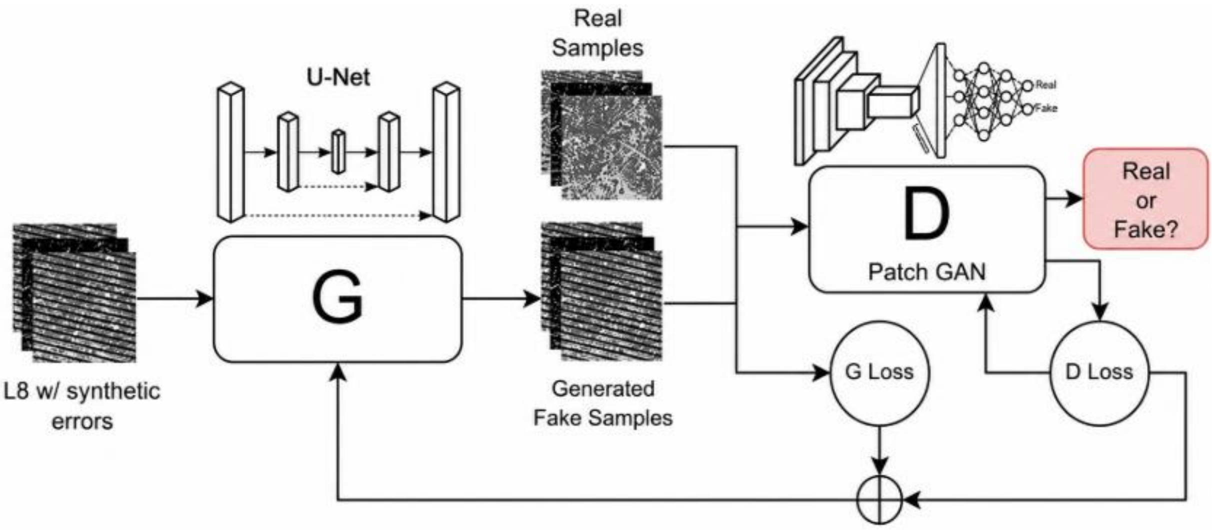

Figure 5.9. Illustration of Pix2Pix architecture [84].

These approaches enable the direct transformation of input fields, such as displacement or strain maps, into corresponding output fields, including thermal distributions or damage indicators. The relevance of encoder–decoder networks to experimental mechanics arises from the structural similarity between experimental measurements and image data.

Full-field measurements obtained from techniques such as Digital Image Correlation and Infrared Thermography can be represented as two-dimensional grids, making them naturally compatible with convolutional architectures. Encoder–decoder models leverage this structure to learn complex, non-linear relationships between different physical fields, enabling data-driven modelling of coupled thermomechanical phenomena.
In the context of this work, encoder–decoder architectures provide a suitable framework for learning mappings between mechanical and thermal fields. By combining hierarchical feature extraction with spatially resolved reconstruction, these models enable the prediction of full-field quantities that are otherwise difficult to measure directly. This capability forms the basis for the integration of experimental mechanics and artificial intelligence, particularly in applications involving data fusion and surrogate modelling [13].

5.4. Image-to-Image Regression

Image-to-image regression represents a class of learning problems in which the objective is to predict a spatially structured output from a corresponding input image. Unlike traditional classification tasks, where the output is a discrete label, image-to-image models operate at the pixel level, learning continuous mappings between input and output domains. This formulation is particularly suitable for applications involving full-field data, where both inputs and outputs can be represented as two-dimensional scalar or vector fields.

In convolutional neural networks, such problems are typically addressed using fully convolutional or encoder–decoder architectures, which preserve spatial structure throughout the network. By avoiding fully connected layers, these models maintain a direct correspondence between input and output locations, enabling dense, pixel-wise prediction[13,80]. This property is essential in experimental mechanics, where spatial relationships reflect underlying physical processes.
A widely adopted framework for image-to-image learning is the use of paired datasets, in which each input image corresponds to a target output image. Supervised learning is then used to minimise a loss function defined over the difference between predicted and reference fields. Conditional generative models, such as pix2pix, extend this concept by incorporating adversarial learning, allowing the network to produce outputs that are not only numerically accurate but also structurally realistic[74]. These models have demonstrated strong performance in a wide range of tasks, including translation between different physical modalities.

The applicability of image-to-image regression to experimental mechanics arises from the structural similarity between measurement fields. Displacement maps, strain fields, and temperature distributions obtained from Digital Image Correlation and Infrared Thermography can all be represented as image-like data. This enables the formulation of problems in which one physical quantity is predicted directly from another, effectively learning a mapping between different measurement modalities.

Recent studies have demonstrated the effectiveness of such approaches in the context of Digital Image Correlation, where convolutional neural networks have been used to estimate displacement and strain fields directly from image data [17,21,22]. Similarly, in thermographic applications, deep learning methods have been employed for defect detection, thermal pattern analysis, and the prediction of temperature distributions under various loading conditions [18,24,25].

Within this context, the combination of Digital Image Correlation and Infrared Thermography represents a particularly suitable application domain. While DIC provides detailed information on displacement and strain fields, thermography captures the associated thermal response related to energy dissipation. Image-to-image regression enables the direct mapping between these domains, allowing the prediction of thermal behaviour from mechanical measurements or vice versa. This approach has been explored in recent work using encoder–decoder and generative architectures, demonstrating the feasibility of learning coupled thermomechanical relationships from experimental data [15,16].

Despite its advantages, image-to-image regression in experimental mechanics presents several challenges. The quality of the learned mapping depends strongly on the availability and representativeness of training data, as well as on the consistency between input and output measurements. Noise, measurement uncertainty, and variations in experimental conditions can significantly affect model performance. Furthermore, while these models can approximate complex relationships, they do not inherently enforce physical laws, which may limit interpretability and generalisation in certain scenarios. These limitations motivate the integration of physics-based constraints and hybrid modelling approaches, which are discussed in subsequent sections [26,27,28].

5.5. Artificial Intelligence Applications in Digital Image Correlation

The integration of artificial intelligence into Digital Image Correlation (DIC) has emerged as a promising direction for improving both the efficiency and robustness of full-field deformation measurements. Traditional DIC methods rely on iterative optimisation procedures to determine displacement fields by maximising correlation between subsets of reference and deformed images. While these approaches are well established, they can be computationally intensive and sensitive to noise, subset selection, and parameter tuning. Recent advances in machine learning, particularly deep learning, have enabled the development of data-driven approaches that aim to overcome some of these limitations, shifting the paradigm from optimisation-based correlation towards learning-based inference of displacement fields [13,29].

A key area of research involves the use of convolutional neural networks (CNNs) to directly estimate displacement and strain fields from image data. In contrast to classical subset-based methods, these approaches learn the mapping between image pairs and the corresponding deformation fields through supervised training. In many implementations, this mapping is realised using encoder–decoder architectures, such as fully convolutional networks and U-Net-based models, which are specifically designed for pixel-wise prediction tasks[70,85]. Furthermore, image-to-image translation frameworks, including conditional generative adversarial networks such as pix2pix [74] and CycleGAN [86], have been successfully applied to learn complex mappings between full-field quantities [74,86]. From a methodological perspective, these approaches are closely related to developments in optical flow and dense image matching, where deep neural networks are used to estimate pixel-wise motion fields directly from image sequences [85,87].

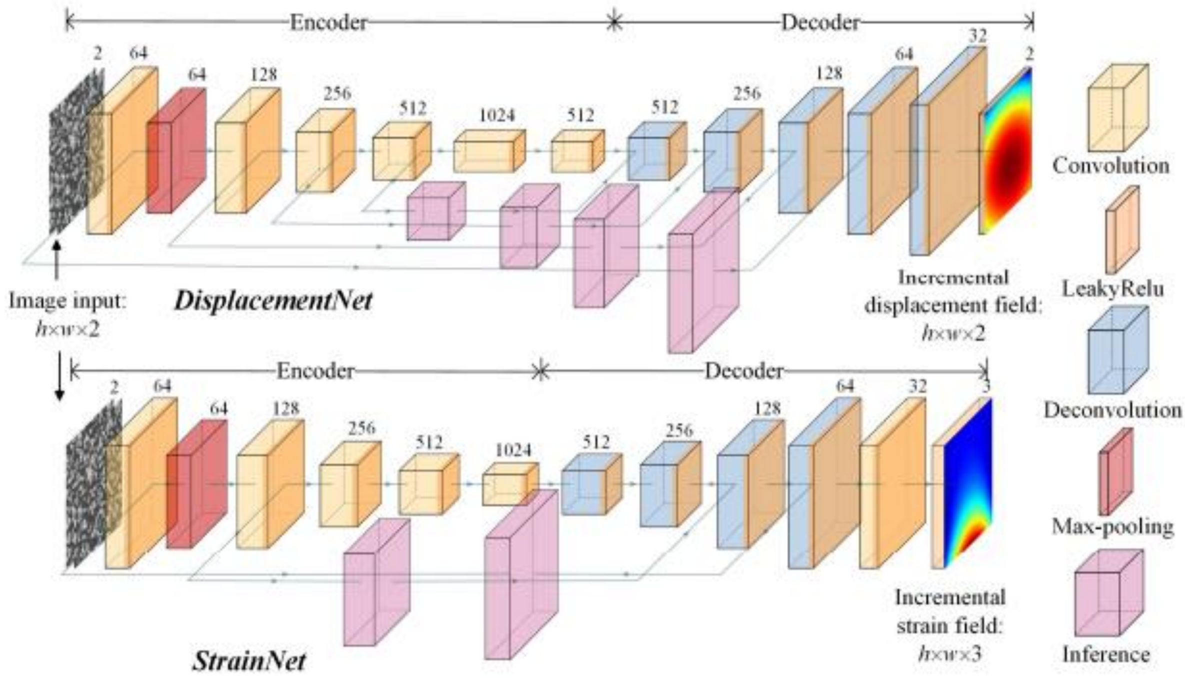

Figure 5.10. CNN architecture of DisplacementNet and StrainNet. The numbers above each module indicate the feature map depth[17].

Such architectures enable end-to-end learning of spatially resolved deformation fields, making them particularly suitable for full-field experimental data, where both local and global deformation patterns must be captured simultaneously [70,85]. This enables rapid inference once the model is trained, significantly reducing computational cost compared to iterative correlation algorithms (see Figure 5.10.) [17,21,23]. Such methods have demonstrated the ability to capture complex deformation patterns while maintaining competitive accuracy, particularly in scenarios where traditional methods struggle due to noise, decorrelation, or poor speckle quality [17,21,23].

From this perspective, modern AI-based DIC methods can be interpreted as image-to-image regression problems, where the objective is to learn a physically meaningful transformation between different representations of deformation fields [21,23]. These approaches are particularly beneficial in experimental conditions with low image quality, non-ideal lighting, or high-speed acquisition, where conventional DIC performance may degrade. By learning statistical patterns in the data, deep learning models can effectively suppress noise and recover meaningful deformation information, consistent with broader applications of machine learning in experimental and computational mechanics [76].

Another important development is the incorporation of physical constraints into neural network-based DIC frameworks. Physics-informed approaches introduce relationships such as strain–displacement compatibility or equilibrium conditions into the learning process, improving the physical consistency of predicted fields [22]. This represents a significant step towards bridging the gap between purely data-driven models and traditional mechanics-based formulations. Hybrid approaches combining classical DIC algorithms with machine learning components have also been proposed, aiming to integrate the robustness of correlation-based methods with the adaptability of data-driven models [17,22,88].

Despite these advances, several challenges remain. The performance of AI-based DIC methods depends strongly on the availability of high-quality training data that adequately represent the range of deformation scenarios encountered in practice. Generalisation to unseen materials, loading conditions, or imaging setups remains a key concern. Furthermore, while deep learning models can provide accurate predictions, their interpretability is often limited compared to traditional methods, making it more difficult to assess the reliability of results in critical applications. These limitations have motivated the development of physics-informed and hybrid modelling strategies that aim to improve generalisation and enforce physical consistency [26,27,28].

Overall, artificial intelligence has the potential to significantly enhance Digital Image Correlation by enabling faster computation, improved robustness, and new capabilities for analysing complex deformation fields. However, careful integration with established experimental and theoretical frameworks is essential to ensure that these methods provide physically meaningful and reliable results.

5.6. Artificial Intelligence Applications in Infrared Thermography

Artificial intelligence has become an increasingly important tool in Infrared Thermography, enabling advanced analysis of thermal data beyond conventional qualitative and quantitative approaches. Traditional thermographic analysis relies on interpreting temperature fields based on visual inspection, thresholding, or simplified analytical models. While effective in controlled scenarios, these methods are often limited in their ability to detect subtle patterns, handle noisy data, or capture complex spatiotemporal behaviour. The introduction of machine learning, particularly deep learning, has significantly expanded the capabilities of thermographic analysis by enabling automated feature extraction and data-driven interpretation of thermal fields.

A major area of application is defect detection (see Figure 5.11.) and material characterisation. Deep learning models, particularly convolutional neural networks, have been successfully applied to identify defects in materials using thermographic data, including pulsed and lock-in thermography. These methods are capable of recognising subtle thermal signatures associated with subsurface defects, cracks, or material inhomogeneities, often outperforming traditional signal processing techniques [18,24,25]. By learning spatial and temporal patterns in thermal data, such models enable more reliable and automated inspection procedures.

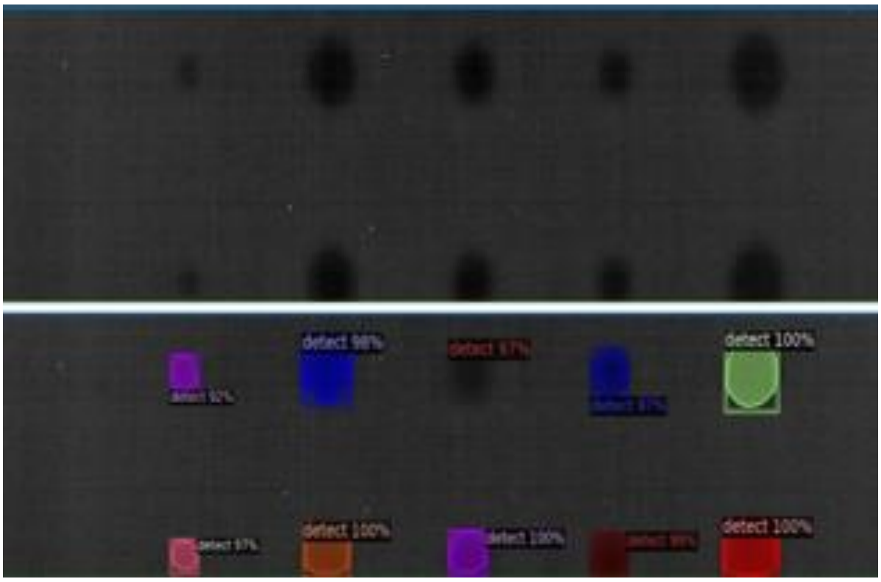

Figure 5.11. Defect detection in material using pulsed thermographic data[24].

In addition to defect detection, AI methods have been employed for thermal pattern analysis and interpretation. Neural networks can extract meaningful features from complex temperature fields, enabling classification of thermal responses, segmentation of regions of interest, and identification of evolving thermal behaviour during loading. Spatiotemporal deep learning approaches, which consider both spatial distribution and temporal evolution of temperature, are particularly effective for analysing transient thermomechanical processes and dynamic experiments [25].

A further important application, particularly relevant to this work, is the prediction of thermal fields from mechanical data. Image-to-image regression frameworks, including encoder–decoder architectures and generative models such as pix2pix [16] and CycleGAN [86], have been used to learn mappings between different physical modalities. In this context, neural networks can be trained to predict temperature distributions directly from displacement or strain fields obtained via Digital Image Correlation. This approach enables data-driven modelling of thermomechanical coupling without explicitly solving governing equations, providing a powerful tool for analysing energy dissipation and deformation processes [15,16].

Despite these advances, several challenges remain. Thermographic data are influenced by factors such as emissivity variations, reflections, environmental conditions, and measurement noise, which can complicate both data acquisition and model training. In addition, the availability of high-quality, synchronised datasets linking thermal and mechanical fields is often limited, which can restrict the performance and generalisation of deep learning models. As with other AI-based approaches, the lack of explicit physical constraints may lead to results that are difficult to interpret or validate in a rigorous mechanical context.

Overall, artificial intelligence significantly enhances the capabilities of Infrared Thermography by enabling automated analysis, improved defect detection, and data-driven modelling of complex thermomechanical phenomena. When combined with complementary techniques such as Digital Image Correlation, AI-based thermographic analysis provides a powerful framework for understanding deformation and energy dissipation in experimental mechanics.

5.7. Current Limitations and Challenges

Despite the rapid progress of artificial intelligence in experimental mechanics, several fundamental challenges remain that limit the widespread adoption and reliability of these approaches. Among the most significant are issues related to generalisation, data dependency, interpretability, and robustness, all of which are particularly critical in the context of full-field measurement techniques such as Digital Image Correlation and Infrared Thermography.

A primary limitation of deep learning-based methods is their strong dependence on training data. The performance of neural networks is inherently tied to the quality, quantity, and diversity of the datasets used during training. In experimental mechanics, obtaining large, well-controlled, and synchronised datasets—particularly those combining multiple measurement modalities such as displacement, strain, and temperature fields—is often challenging. As a result, trained models may perform well under conditions similar to those seen during training, but their ability to generalise to new materials, geometries, loading conditions, or experimental setups remains limited. This issue is especially pronounced in applications involving complex thermomechanical coupling, where the underlying physical relationships may vary significantly across different scenarios [26,27,28].

Closely related to data dependency is the challenge of generalisation. Unlike traditional mechanics-based approaches, which rely on physically grounded models, data-driven methods learn implicit relationships from observations. While this allows them to capture complex behaviours without explicitly defining governing equations, it also means that extrapolation beyond the training domain is inherently uncertain. In practice, even small variations in imaging conditions, speckle patterns, emissivity, or noise characteristics can lead to degradation in model performance. These limitations highlight the importance of carefully designed datasets and motivate the development of hybrid approaches that combine data-driven learning with physical constraints.

Another important challenge concerns interpretability. Deep neural networks are often treated as black-box models, providing limited insight into how predictions are generated. In experimental mechanics, where measurements are frequently used to support engineering decisions, the ability to interpret and validate results is essential. The lack of transparency in AI-based methods can make it difficult to assess whether predictions are physically meaningful or whether they arise from spurious correlations in the data. Although recent advances in explainable artificial intelligence have provided tools for analysing learned features and model behaviour, their application in the context of full-field experimental data remains limited [20].

Robustness is also a critical concern. Experimental data are inherently subject to noise, measurement uncertainty, and variations in acquisition conditions. While deep learning models can be trained to handle certain types of noise, their performance may degrade significantly when exposed to conditions that differ from those encountered during training. This includes variations in lighting, surface preparation, camera calibration, or environmental influences. In addition, the presence of artefacts in thermographic data, such as reflections or emissivity variations, can further complicate model predictions and reduce reliability.

Finally, although significant progress has been made in applying artificial intelligence to individual measurement modalities, the integration of multiple full-field data sources within a unified learning framework remains relatively underexplored. In particular, approaches that directly link mechanical fields obtained from Digital Image Correlation with thermal fields measured via Infrared Thermography are still limited in the literature. This highlights an important research direction, where combining complementary measurement techniques with data-driven models may provide deeper insight into thermomechanical behaviour and energy dissipation processes.

In summary, while artificial intelligence offers powerful tools for analysing full-field experimental data, its application in experimental mechanics is still accompanied by important challenges related to data availability, generalisation, interpretability, and robustness. Addressing these limitations through improved datasets, physics-informed modelling, and multimodal data integration will be essential for the reliable and widespread adoption of these methods.

6. Conclusion

Based on the reviewed literature, it can be concluded that Digital Image Correlation and Infrared Thermography should not be regarded only as separate full-field measurement techniques, but also as complementary descriptions of the same thermomechanical response. DIC provides detailed information on displacement and strain fields, while IRT captures temperature changes associated with thermoelastic effects, plastic dissipation, and damage-related heat generation. When these measurements are analysed independently, the connection between deformation and heat generation may remain only partially understood. Therefore, a more integrated interpretation of mechanical and thermal fields appears necessary for a more complete analysis of complex material behaviour in experimental mechanics.

From this perspective, artificial intelligence represents a relevant tool for extending the interpretation of full-field experimental data. The reviewed studies show that deep learning methods are already capable of processing image-like mechanical and thermal fields, reducing noise, estimating displacement or strain, and identifying thermal patterns. However, the direct data-driven connection between DIC and IRT remains insufficiently developed. This indicates that the combination of DIC, IRT, and artificial intelligence is not only a relevant direction, but also a scientifically justified approach for analysing coupled thermomechanical phenomena.

The reviewed literature indicates that the main value of such approaches lies in their ability to connect measurements that are physically related but experimentally difficult to combine. This is particularly important in dynamic testing, impact loading, and experiments with restricted optical or thermal access, where one measurement modality may be incomplete, noisy, or unavailable. Data-driven mapping between mechanical and thermal fields may therefore contribute to a more efficient use of experimental data and support the reconstruction or interpretation of quantities that cannot always be measured directly.

Future work in this area should place strong emphasis on physical consistency, experimental validation, and model generalisation. The development of reliable data-driven methods requires representative paired datasets, careful assessment of uncertainty, and validation across different materials, geometries, and loading conditions. In addition to direct mapping between DIC and IRT measurements, further research may include physics-informed learning, hybrid experimental–numerical approaches, and comparison with finite element or analytical thermomechanical models. Standardised paired DIC–IRT datasets and benchmark problems would also support more reliable evaluation and comparison of different data-driven methods. Furthermore, temporal modelling of full-field measurements may provide additional insight into the evolution of deformation, heat generation, and damage mechanisms during complex loading processes.

Without these aspects, artificial intelligence models risk remaining purely numerical tools with limited physical relevance. For this reason, the integration of DIC, IRT, and artificial intelligence should be understood as a complementary extension of experimental mechanics, rather than a replacement for established measurement methods. Such approaches are most valuable when they support physical interpretation, improve the use of available experimental data, and provide additional insight into quantities or relationships that are difficult to access through conventional measurement or numerical modelling alone.

Overall, the reviewed material shows that combining Digital Image Correlation, Infrared Thermography, and artificial intelligence provides a promising pathway toward more complete full-field analysis of material behaviour. Such integration may improve the interpretation of thermomechanical coupling, support the analysis of complex and inaccessible experimental conditions, and contribute to the development of more adaptive, validated, and physically informed methodologies in experimental mechanics.

7. References

1. Sutton, M.A.; Wolters, W.J.; Peters, W.H.; Ranson, W.F.; McNeill, S.R. Determination of Displacements Using an Improved Digital Correlation Method. *Image Vis. Comput.* **1983**, *1*, 133–139, doi:https://doi.org/10.1016/0262-8856(83)90064-1.
2. Orteu, M.A.; Schreier, J.J.; Springer, H. Image Correlation for Shape, Motion and Deformation Measurements.; Springer, 2009.
3. Schreier, H.W.; Sutton, M.A. Systematic Errors in Digital Image Correlation Due to Undermatched Subset Shape Functions. *Exp. Mech.* **2002**, *42*, 303–310, doi:10.1007/BF02410987.
4. Pitarresi, G.; Patterson, E.A. A Review of the General Theory of Thermoelastic Stress Analysis. *J. Strain Anal. Eng. Des.* **2003**, *38*, 405–417, doi:10.1243/03093240360713469.
5. Krstlović-Opara, L.; Surjak, M.; Vesenjak, M.; Tonković, Z.; Frančeski, J.; Kodvanj, J.; Domazet, Ž. Determination of Material Properties Using Dynamic Tests Supported by Thermography, Digital Image Correlation and Numerical Simulation. In Proceedings of the 8th International Congress of Croatian Society of Mechanics; 2015; p. 53.
6. Xavier P. Maldague *Theory and Practice of Infrared Technology for Nondestructive Testing*; 1st ed.; Wiley, 2001; Vol. 1;.
7. Usamentiaga, R.; Venegas, P.; Guerediaga, J.; Vega, L.; Molleda, J.; Bulnes, F.G. Infrared Thermography for Temperature Measurement and Non-Destructive Testing. *Sensors* **2014**, *14*, 12305–12348, doi:10.3390/s140712305.
8. Chrysochoos, A. Infrared Thermography Applied to the Analysis of Material Behavior: A Brief Overview. *Quant. Infrared Thermogr. J.* **2012**, *9*, 193–208, doi:10.1080/17686733.2012.746069.
9. Kaplan, H. Practical Applications of Infrared Thermal Sensing and Imaging Equipment. **2007**, doi:10.1117/3.725072.
10. Bagavathiappan, S.; Lahiri, B.B.; Saravanan, T.; Philip, J.; Jayakumar, T. Infrared Thermography for Condition Monitoring – A Review. *Infrared Phys. Technol.* **2013**, *60*, 35–55, doi:https://doi.org/10.1016/j.infrared.2013.03.006.
11. Novak, N.; Krstulović-Opara, L.; Ren, Z.; Vesenjak, M. Compression and Shear Behaviour of Graded Chiral Auxetic Structures. *Mechanics of Materials* **2020**, *148*, 103524, doi:10.1016/J.MECHMAT.2020.103524.
12. Novak, N.; Vesenjak, M.; Krstulović-Opara, L.; Ren, Z. Mechanical Characterisation of Auxetic Cellular Structures Built from Inverted Tetrapods. *Compos. Struct.* **2018**, *196*, 96–107, doi:https://doi.org/10.1016/j.compstruct.2018.05.024.
13. Goodfellow, I.; Bengio, Y.; Courville, A. *Deep Learning*; MIT Press, 2016;
14. LeCun, Y.; Bengio, Y.; Hinton, G. Deep Learning. *Nature* **2015**, *521*, 436–444, doi:10.1038/nature14539.
15. Grebo, A.; Novak, N.; Panić, B.; Krstulović-Opara, L. A Deep Learning Framework for Full-Field Thermal Field Distribution Prediction from Digital Image Correlation Strain Measurements. *Applied Sciences* **2026**, *16*, doi:10.3390/app16010460.
16. Grebo, A.; Krstulović-Opara, L.; Domazet, Ž. Thermal to Digital Image Correlation Image to Image Translation with CycleGAN and Pix2Pix. *Mater. Today Proc.* **2023**, *93*, 752–760, doi:https://doi.org/10.1016/j.matpr.2023.06.219.
17. Yang, R.; Li, Y.; Zeng, D.; Guo, P. Deep DIC: Deep Learning-Based Digital Image Correlation for End-to-End Displacement and Strain Measurement. *J. Mater. Process. Technol.* **2022**, *302*, 117474, doi:10.1016/J.JMATPROTEC.2021.117474.

18. Cha, Y.; Yun, H.; Cho, S.; Chung, W. Deep Learning-Assisted Thermal Image Analysis for Assessment of Cementitious Composite Flaws. *Case Studies in Construction Materials* **2025**, *23*, e05161, doi:10.1016/J.CSCM.2025.E05161.
19. Rosa, R.G.; Barella, B.P.; Vargas, I.G.; Tarpani, J.R.; Herrmann, H.-G.; Fernandes, H. Advanced Thermal Imaging Processing and Deep Learning Integration for Enhanced Defect Detection in Carbon Fiber-Reinforced Polymer Laminates. *Materials* **2025**, *18*, doi:10.3390/ma18071448.
20. Samek, W.; Wiegand, T.; Müller, K.-R. Explainable Artificial Intelligence: Understanding, Visualizing and Interpreting Deep Learning Models. *CoRR* **2017**, *abs/1708.08296*.
21. Duan, X.; Xu, H.; Dong, R.; Lin, F.; Huang, J. Digital Image Correlation Based on Convolutional Neural Networks. *Opt. Lasers Eng.* **2023**, *160*, 107234, doi:10.1016/J.OPTLASENG.2022.107234.
22. Cheng, X.; Zhou, S.; Xing, T.; Zhu, Y.; Ma, S. Solving Digital Image Correlation with Neural Networks Constrained by Strain-Displacement Relations. *Opt. Express* **2023**, *31*, 3865–3880, doi:10.1364/OE.475232.
23. Niu, B.; Ji, J. Convolutional Neural Network Based Denoising for Digital Image Correlation Reconstructing High-Fidelity Deformation Field. In Proceedings of the 2023 IEEE/ASME International Conference on Advanced Intelligent Mechatronics (AIM); IEEE, June 28 2023; pp. 727–732.
24. Fang, Q.; Ibarra-Castanedo, C.; Garrido, I.; Duan, Y.; Maldague, X. Automatic Detection and Identification of Defects by Deep Learning Algorithms from Pulsed Thermography Data. *Sensors* **2023**, *23*, doi:10.3390/s23094444.
25. Schmid, S.; Reinhardt, J.; Grosse, C.U. Spatial and Temporal Deep Learning for Defect Detection with Lock-in Thermography. *NDT & E International* **2024**, *143*, 103063, doi:10.1016/J.NDTEINT.2024.103063.
26. Raissi, M.; Perdikaris, P.; Karniadakis, G.E. Physics-Informed Neural Networks: A Deep Learning Framework for Solving Forward and Inverse Problems Involving Nonlinear Partial Differential Equations. *J. Comput. Phys.* **2019**, *378*, 686–707, doi:10.1016/j.jcp.2018.10.045.
27. Karniadakis, G.E.; Kevrekidis, I.G.; Lu, L.; Perdikaris, P.; Wang, S.; Yang, L. Physics-Informed Machine Learning. *Nature Reviews Physics* **2021**, *3*, 422–440, doi:10.1038/s42254-021-00314-5.
28. Willard, J.; Jia, X.; Xu, S.; Steinbach, M.; Kumar, V. Integrating Scientific Knowledge with Machine Learning for Engineering and Environmental Systems 2022.
29. Pan, B.; Qian, K.; Xie, H.; Asundi, A. Two-Dimensional Digital Image Correlation for in-Plane Displacement and Strain Measurement: A Review. *Meas. Sci. Technol.* **2009**, *20*, 62001, doi:10.1088/0957-0233/20/6/062001.
30. Jones, A.; DiCecco, S.; Furmanski, J.; Harmon, B.; Koohbor, B.; Mathieu, F.; Blaysat, B.; Coret, M.; Hild, F.; Lava, P.; et al. *A Good Practices Guide for Digital Image Correlation*; 2025;
31. Novak, N.; Grebo, A.; Borovinšek, M.; Krstulović-Opara, L.; Ren, Z.; Vesenjak, M. Deformation Behaviour of Optimised Three-Dimensional Axisymmetric Chiral Auxetic Structures. *Biomedicines* **2025**, *13*, 2816, doi:10.3390/biomedicines13112816.
32. Turner, D.Z. Digital Image Correlation Engine (DICe) Reference Manual. *Sandia report, Sand2015-10606 O* **2015**.
33. Blaber, J.; Adair, B.; Antoniou, A. Ncorr: Open-Source 2D Digital Image Correlation Matlab Software. *Exp. Mech.* **2015**, *55*, 1105–1122, doi:10.1007/s11340-015-0009-1.
34. Gorjup Domen, S.J. Ladisk / PyDIC.

35. Yang, J.; Bhattacharya, K. Augmented Lagrangian Digital Image Correlation. *Exp. Mech.* **2019**, *59*, 187–205, doi:10.1007/s11340-018-00457-0.
36. Hild, F.; Roux, S. Digital Image Correlation: From Displacement Measurement to Identification of Elastic Properties - A Review. *Strain* **2005**, *42*, doi:10.1111/j.1475-1305.2006.00258.x.
37. Bruck, H.A.; McNeill, S.R.; Sutton, M.A.; Peters, W.H. Digital Image Correlation Using Newton-Raphson Method of Partial Differential Correction. *Exp. Mech.* **1989**, *29*, 261–267, doi:10.1007/BF02321405.
38. Schreier, H.W.; Garcia, D.; Sutton, M.A. Advances in Light Microscope Stereo Vision. *Exp. Mech.* **2004**, *44*, 278–288, doi:10.1007/BF02427894.
39. Schreier, H.W.; Braasch, J.R.; Sutton, M.A. Systematic Errors in Digital Image Correlation Caused by Intensity Interpolation. *Optical Engineering* **2000**, *39*, 2915 – 2921, doi:10.1117/1.1314593.
40. Lecompte, D.; Smits, A.; Bossuyt, S.; Sol, H.; Vantomme, J.; Van Hemelrijck, D.; Habraken, A.M. Quality Assessment of Speckle Patterns for Digital Image Correlation. *Opt. Lasers Eng.* **2006**, *44*, 1132–1145, doi:10.1016/j.optlaseng.2005.10.004.
41. Hild, F.; Roux, S. Comparison of Local and Global Approaches to Digital Image Correlation. *Exp. Mech.* **2012**, *52*, 1503–1519, doi:10.1007/s11340-012-9603-7.
42. Sutton, M.A.; Turner, J.L.; Bruck, H.A.; Chae, T.A. Full-Field Representation of Discretely Sampled Surface Deformation for Displacement and Strain Analysis. *Exp. Mech.* **1991**, *31*, 168–177, doi:10.1007/BF02327571.
43. Jiang, Z. OpenCorr: An Open Source Library for Research and Development of Digital Image Correlation. *Opt. Lasers Eng.* **2023**, *165*, 107566, doi:10.1016/j.optlaseng.2023.107566.
44. O. C. Zienkiewicz; R. L. Taylor; J.Z. Zhu *The Finite Element Method: Its Basis and Fundamentals*; Elsevier, 2013; ISBN 9781856176330.
45. Zaplatić, A.; Tomičević, Z.; Chang, X.; Kosec, P.; Roux, S.; Hild, F. Advanced FE-Based Multimodal Correlation Analyses for the Characterization of Woven Composite. *Mech. Syst. Signal Process.* **2025**, *224*, 112079, doi:10.1016/j.ymssp.2024.112079.
46. Buljac, A.; Jailin, C.; Mendoza, A.; Neggers, J.; Taillandier-Thomas, T.; Bouterf, A.; Smaniotto, B.; Hild, F.; Roux, S. Digital Volume Correlation: Review of Progress and Challenges. *Exp. Mech.* **2018**, *58*, 661–708, doi:10.1007/s11340-018-0390-7.
47. Batra, R.C. *Elements of Continuum Mechanics*; Aiaa, 2006;
48. Jaminion, S.; Nelson, N.W.; Chambard, J.P.; Swiergel, N.; Hild, F. Correli: A Global Approach in Digital Image Correlation. In *International Digital Imaging Correlation Society*; River Publishers: New York, 2025; pp. 277–279.
49. Will LePage Digitalimagecorrelation.Org.
50. Michael Vollmer, K.-P.M. Fundamentals of Infrared Thermal Imaging. In *Infrared Thermal Imaging: Fundamentals, Research and Applications*; John Wiley & Sons, Ltd, 2017; pp. 1–106 ISBN 9783527693306.
51. Dulieu-Barton, J.M.; Stanley, P. Development and Applications of Thermoelastic Stress Analysis. *J. Strain Anal. Eng. Des.* **1998**, *33*, 93–104, doi:10.1243/0309324981512841.
52. Maldague, X. Nondestructive Evaluation of Materials by Infrared Thermography.; 1993.
53. Chrysochoos, A. Infrared Thermography Applied to the Analysis of Material Behavior: A Brief Overview. *Quant. Infrared Thermogr. J.* **2012**, *9*, 193–208, doi:10.1080/17686733.2012.746069.
54. Minkina, W.; Dudzik, S. *Infrared Thermography*; Wiley, 2009; ISBN 9780470747186.

55. Boulanger, T. Calorimetric Analysis of Dissipative and Thermoelastic Effects Associated with the Fatigue Behavior of Steels. *Int. J. Fatigue* **2004**, *26*, 221–229, doi:10.1016/S0142-1123(03)00171-3.
56. Rittel, D. On the Conversion of Plastic Work to Heat during High Strain Rate Deformation of Glassy Polymers. *Mechanics of Materials* **1999**, *31*, 131–139, doi:10.1016/S0167-6636(98)00063-5.
57. Siegel, R.; Howell, J. Thermal Radiation Heat Transfer. **1972**, *4*.
58. Holst, G.C. *Common Sense Approach to Thermal Imaging*; SPIE, 2000; ISBN 9780819437228.
59. Markus Tarin Thermal Imaging Takes the Temperature of New Applications.
60. Rogalski, A. Infrared Detectors: Status and Trends. *Prog. Quantum Electron.* **2003**, *27*, 59–210, doi:10.1016/S0079-6727(02)00024-1.
61. Budzier, H.& G.G. *Thermal Infrared Remote Sensing*; Kuenzer, C., Dech, S., Eds.; Springer Netherlands: Dordrecht, 2013; Vol. 17; ISBN 978-94-007-6638-9.
62. Neves, A.; Ribeiro, R. Algorithms for Face Detection on Infrared Thermal Images. *International Journal on Advances in Software* **2018**, *10*, 499–512.
63. JPNU What Is NETD of Infrared Thermal Imaging?
64. Taylor, G.I.; Quinney, H. The Latent Energy Remaining in a Metal after Cold Working. *Proceedings of the Royal Society of London. Series A, Containing Papers of a Mathematical and Physical Character* **1934**, *143*, 307–326, doi:10.1098/rspa.1934.0004.
65. Chrysochoos, A. Thermomechanical Analysis of the Cyclic Behavior of Materials. *Procedia IUTAM* **2012**, *4*, 15–26, doi:10.1016/j.piutam.2012.05.003.
66. Breitenstein, O.; Langenkamp, M. *Lock-in Thermography*; Springer Berlin Heidelberg: Berlin, Heidelberg, 2003; Vol. 10; ISBN 978-3-642-07785-2.
67. Bagavac, P.; Krstulović-Opara, L.; Domazet, Ž. Pulse Phase Thermography: Impact Damage Retrieval. *Mater. Today Proc.* **2018**, *5*, 26578–26583, doi:10.1016/j.matpr.2018.08.119.
68. La Rosa, G. Thermographic Methodology for Rapid Determination of the Fatigue Limit of Materials and Mechanical Components. *Int. J. Fatigue* **2000**, *22*, 65–73, doi:10.1016/S0142-1123(99)00088-2.
69. Fargione, G. Rapid Determination of the Fatigue Curve by the Thermographic Method. *Int. J. Fatigue* **2002**, *24*, 11–19, doi:10.1016/S0142-1123(01)00107-4.
70. Ronneberger Olaf and Fischer, P. and B.T. U-Net: Convolutional Networks for Biomedical Image Segmentation. In Proceedings of the Medical Image Computing and Computer-Assisted Intervention – MICCAI 2015; Navab Nassir and Hornegger, J. and W.W.M. and F.A.F., Ed.; Springer International Publishing: Cham, 2015; pp. 234–241.
71. Huo, W.; Bakir, N.; Gumenyuk, A.; Rethmeier, M.; Wolter, K. Strain Prediction Using Deep Learning during Solidification Crack Initiation and Growth in Laser Beam Welding of Thin Metal Sheets. *Applied Sciences* **2023**, *13*, doi:10.3390/app13052930.
72. Tabernik, D.; Šela, S.; Skvarč, J.; Skočaj, D. Segmentation-Based Deep-Learning Approach for Surface-Defect Detection. *J. Intell. Manuf.* **2019**, *31*, 759–776, doi:10.1007/s10845-019-01476-x.
73. Roy, S.; Yogi, B.; Majumdar, R.; Ghosh, P.; Das, S.K. Deep Learning-Based Crack Detection and Prediction for Structural Health Monitoring. *Discover Applied Sciences* **2025**, *7*, 674, doi:10.1007/s42452-025-07272-y.
74. Isola, P.; Zhu, J.-Y.; Zhou, T.; Efros, A.A. Image-to-Image Translation with Conditional Adversarial Networks. *CoRR* **2016**, *abs/1611.07004*.
75. Yosinski, J.; Clune, J.; Bengio, Y.; Lipson, H. How Transferable Are Features in Deep Neural Networks? *CoRR* **2014**, *abs/1411.1792*.

76. Brunton, S.L.; Noack, B.R.; Koumoutsakos, P. Machine Learning for Fluid Mechanics. *Annu. Rev. Fluid Mech.* **2020**, *52*, 477–508, doi:10.1146/annurev-fluid-010719-060214.
77. Zeiler, M.D.; Fergus, R. Visualizing and Understanding Convolutional Networks. *CoRR* **2013**, *abs/1311.2901*.
78. Oquab, M.; Bottou, L.; Laptev, I.; Sivic, J. Learning and Transferring Mid-Level Image Representations Using Convolutional Neural Networks. In Proceedings of the 2014 IEEE Conference on Computer Vision and Pattern Recognition; 2014; pp. 1717–1724.
79. Zanin, M.; Aitya, N.A.A.; Basilio, J.; Baumbach, J.; Benis, A.; Behera, C.K.; Bucholc, M.; Castiglione, F.; Chouvarda, I.; Comte, B.; et al. An Early Stage Researcher's Primer on Systems Medicine Terminology. *Netw. Syst. Med.* **2021**, *4*, 2–50, doi:10.1089/nsm.2020.0003.
80. Long, J.; Shelhamer, E.; Darrell, T. Fully Convolutional Networks for Semantic Segmentation. In Proceedings of the 2015 IEEE Conference on Computer Vision and Pattern Recognition (CVPR); IEEE, June 2015; pp. 3431–3440.
81. Hinton, G.E.; Salakhutdinov, R.R. Reducing the Dimensionality of Data with Neural Networks. *Science (1979).* **2006**, *313*, 504–507, doi:10.1126/science.1127647.
82. Dinesh Sivakumar Putting Encoder - Decoder Together.
83. Francois Chollet Building Autoencoders in Keras.
84. Adıyaman, H.; Emre Varul, Y.; Bakırman, T.; Bayram, B. Stripe Error Correction for Landsat-7 Using Deep Learning. *PFG – Journal of Photogrammetry, Remote Sensing and Geoinformation Science* **2025**, *93*, 51–63, doi:10.1007/s41064-024-00306-x.
85. Fischer, P.; Dosovitskiy, A.; Ilg, E.; Häusser, P.; Hazırbaş, C.; Golkov, V.; van der Smagt, P.; Cremers, D.; Brox, T. FlowNet: Learning Optical Flow with Convolutional Networks. **2015**.
86. Zhu, J.-Y.; Park, T.; Isola, P.; Efros, A.A. Unpaired Image-to-Image Translation Using Cycle-Consistent Adversarial Networks 2020.
87. Ilg, E.; Mayer, N.; Saikia, T.; Keuper, M.; Dosovitskiy, A.; Brox, T. FlowNet 2.0: Evolution of Optical Flow Estimation with Deep Networks. In Proceedings of the 2017 IEEE Conference on Computer Vision and Pattern Recognition (CVPR); IEEE, July 2017; pp. 1647–1655.
88. Wang, X.; Jiang, G.; Hu, J.; Sfarra, S.; Mostacci, M.; Kouis, D.; Yang, D.; Fernandes, H.; Avdelidis, N.P.; Maldague, X.; et al. Automatic Defect Detection in Infrared Thermal Images of Ancient Polyptychs Based on Numerical Simulation and a New Efficient Channel Attention Mechanism Aided Faster R-CNN Model. *Herit. Sci.* **2024**, *12*, 329, doi:10.1186/s40494-024-01441-9.

8. Abstract

Full-field measurement techniques and artificial intelligence-based approaches are reviewed in the context of experimental mechanics, with emphasis on Digital Image Correlation (DIC), Infrared Thermography (IRT), and data-driven interpretation of coupled thermomechanical behaviour. Digital Image Correlation provides non-contact measurement of displacement and strain fields by analysing changes in image intensity between reference and deformed states, while Infrared Thermography enables measurement of temperature fields by detecting thermal radiation emitted from the material surface. Although both methods are widely used in experimental mechanics, they are commonly applied and interpreted separately, which may limit the understanding of the relationship between deformation, heat generation, and damage development.

The fundamental principles of local Digital Image Correlation, infrared thermography, thermomechanical material response, and heat dissipation during deformation are reviewed. Recent applications of machine learning and deep learning in the analysis of full-field experimental data are also discussed, with particular attention given to convolutional neural networks, encoder–decoder architectures, image-to-image regression, and multimodal data analysis. The reviewed studies show that artificial intelligence methods have already been applied to DIC and IRT separately for tasks such as displacement and strain estimation, noise reduction, defect detection, and thermal pattern interpretation. However, direct data-driven mapping between DIC-derived mechanical fields and IRT-based thermal fields remains comparatively underexplored.

Based on the reviewed literature, the integration of DIC, IRT, and artificial intelligence is identified as a promising direction for improving the interpretation of coupled thermomechanical phenomena. Such approaches may support the analysis of experimentally limited or inaccessible quantities, especially in dynamic testing, impact loading, and conditions involving restricted optical or thermal access. Future developments in this field should place emphasis on physical consistency, experimental validation, uncertainty assessment, representative paired datasets, and comparison with numerical or analytical thermomechanical models. Overall, the reviewed material indicates that data-driven full-field analysis can complement established experimental techniques and contribute to more adaptive, efficient, and physically informed methodologies in experimental mechanics.

9. Prošireni sažetak

U eksperimentalnoj mehanici sve se više koriste punopoljne (engl. full-field) mjerne metode koje omogućuju detaljan uvid u ponašanje materijala i konstrukcija tijekom mehaničkog opterećenja. Za razliku od klasičnih mjernih tehnika, poput tenzometara ili termoparova, koje pružaju informacije samo u pojedinim točkama, punopoljne metode omogućuju kontinuirani prikaz raspodjele deformacija, pomaka i temperature na cijelom području ispitivanja. Takav pristup posebno je važan kod analize složenih mehaničkih pojava kao što su lokalizacija deformacija, inicijacija i propagacija oštećenja, pojava pukotina te različiti nelinearni procesi koji se javljaju pri statičkom, dinamičkom ili udarnom opterećenju. Upravo zbog mogućnosti detaljnog prostornog prikaza mehaničkog odziva, punopoljne metode danas imaju značajnu ulogu u istraživanju naprednih materijala, kompozita, celularnih i auxetic struktura te drugih složenih inženjerskih sustava.

Među najčešće korištenim punopoljnim metodama ističu se Korelacija Digitalne Slike (DIC) i infracrvena termografija (IRT). Korelacija Digitalne Slike predstavlja optičku, beskontaktnu metodu kojom se određuju polja pomaka i deformacija na površini ispitivanog tijela. Metoda se temelji na praćenju slučajnog uzorka nanesenog na površinu ispitivanog tijela tijekom deformacije. Analizom promjena sivinskih vrijednosti (engl. grayscale intensity values) između referentnog i deformiranog stanja moguće je odrediti pomake pojedinih dijelova slike, a zatim i deformacijska polja. U lokalnom pristupu (engl. local DIC) analiza se provodi na manjim područjima slike, odnosno podskupovima, pri čemu se svaki podskup obrađuje neovisno. Takav pristup omogućuje vrlo visoku prostornu rezoluciju i dobro praćenje lokalnih deformacijskih pojava, uključujući koncentracije deformacija i inicijaciju oštećenja. Međutim, određivanje deformacija temelji se na numerički izračunatom polju pomaka, zbog čega rezultati mogu biti osjetljivi na šum i kvalitetu slike. To zahtijeva pažljiv odabir parametara korelacije, kvalitete uzorka i uvjeta osvjetljenja kako bi se osigurala pouzdanost mjerenja.

Infracrvena termografija predstavlja drugu važnu punopoljnu metodu koja omogućuje mjerenje temperaturnih polja detekcijom infracrvenog zračenja koje emitira promatrano tijelo. Budući da sva tijela temperature iznad apsolutne nule emitiraju toplinsko zračenje, infracrvene kamere mogu beskontaktno pratiti raspodjelu temperature na površini materijala. U eksperimentalnoj mehanici temperaturne promjene često su izravno povezane s termomehaničkim procesima unutar materijala. Tijekom elastične deformacije pojavljuju se male i reverzibilne promjene temperature povezane s termoelastičnim efektom, dok pri plastičnoj deformaciji dolazi do disipacije mehaničke energije u obliku topline. Dio plastičnog rada pretvara se u toplinsku energiju, što rezultira lokalnim porastom temperature koji se može registrirati infracrvenom kamerom. Ova povezanost često se opisuje Taylor–Quinneyjevim koeficijentom, koji predstavlja omjer između plastičnog rada i generirane topline. Zbog toga infracrvena termografija omogućuje neizravan uvid u procese disipacije energije, lokalizacije deformacija i nastanka oštećenja.

Iako su Korelacija Digitalne Slike i infracrvena termografija iznimno raširene metode, u praksi se najčešće koriste odvojeno. Time se gubi dio informacije o međusobnoj povezanosti mehaničkih i toplinskih polja, iako su ona posljedica istog fizikalnog procesa. Polja deformacija i temperaturna polja predstavljaju različite manifestacije ponašanja materijala tijekom opterećenja. Mehanički rad, disipacija energije i toplinski odziv međusobno su povezani, no klasični pristupi često ih analiziraju neovisno. Ograničenja postaju još izraženija u složenijim eksperimentalnim uvjetima, primjerice kod visokobrzinskih i udarnih ispitivanja. U takvim uvjetima infracrvena mjerenja mogu biti otežana zbog zaštitnih konstrukcija, ograničenog optičkog pristupa ili smanjene prostorne i vremenske rezolucije infracrvenih kamera. Osim toga, refleksije, promjene emisivnosti i šum dodatno mogu otežati interpretaciju termografskih podataka.

Razvoj umjetne inteligencije, posebice metoda strojnog i dubokog učenja, otvorio je nove mogućnosti u obradi i interpretaciji eksperimentalnih podataka. Konvolucijske neuronske mreže pokazale su se posebno učinkovitima u analizi slikovnih podataka jer omogućuju automatsko izdvajanje značajki i učenje složenih nelinearnih odnosa između ulaznih i izlaznih veličina. Za razliku od klasičnih pristupa, kod kojih je potrebno ručno definirati značajke i parametre modela, duboke neuronske mreže same uče relevantne obrasce iz podataka tijekom procesa treniranja. U području Korelacije Digitalne Slike metode dubokog učenja koriste se za procjenu polja pomaka i deformacija, smanjenje šuma, ubrzanje obrade podataka i poboljšanje točnosti mjerenja. U infracrvenoj termografiji umjetna inteligencija primjenjuje se za detekciju oštećenja, klasifikaciju toplinskih obrazaca i analizu temperaturnih polja.

Poseban interes predstavlja pristup temeljen na preslikavanju između različitih punopoljnih podataka, pri čemu se uči odnos između dvaju fizikalnih polja. Arhitekture poput enkoder–dekoder modela, među kojima je jedan od najpoznatijih U-Net, omogućuju očuvanje prostorne strukture podataka i generiranje izlaza iste dimenzije kao ulaz. Takvi modeli posebno su prikladni za zadatke prevođenja slike u sliku (engl. image-to-image translation), gdje se jedno polje pokušava predvidjeti na temelju drugoga. U kontekstu eksperimentalne mehanike to znači da se može razmatrati veza između polja deformacija dobivenih metodom Korelacije Digitalne Slike i temperaturnih polja izmjerenih infracrvenom termografijom. Time se otvara mogućnost podatkovno vođene analize povezanosti toplinskog i mehaničkog odziva materijala.

Unatoč značajnom napretku u primjeni umjetne inteligencije, izravno povezivanje DIC i IRT mjerenja još uvijek je relativno slabo istraženo, posebno u području punopoljnih mjerenja u eksperimentalnoj mehanici. Većina postojećih istraživanja usmjerena je ili na mehanička ili na toplinska polja, dok je broj radova koji razmatraju njihovo povezivanje unutar jedinstvenog podatkovno vođenog okvira još uvijek ograničen. Upravo se u tome ističe znanstvena i stručna relevantnost prikazanog pregleda.

Na temelju prikazanih spoznaja, prikazani pregled naglašava važnost povezivanja Korelacije Digitalne Slike, infracrvene termografije i metoda umjetne inteligencije u analizi punopoljnih eksperimentalnih podataka. Pregled pokazuje da kombinacija navedenih metoda predstavlja relevantan smjer za razumijevanje spregnutih termomehaničkih pojava, osobito u kontekstu disipacije energije, lokalizacije deformacija i složenih uvjeta opterećenja. Takav pristup može pridonijeti učinkovitijoj interpretaciji eksperimentalnih mjerenja te pružiti osnovu za daljnje istraživanje podatkovno vođenih metoda u eksperimentalnoj mehanici.

Zaključno, povezivanje Korelacije Digitalne Slike, infracrvene termografije i metoda umjetne inteligencije predstavlja logičan i perspektivan smjer razvoja suvremene eksperimentalne mehanike. Integracija ovih pristupa omogućuje napredniju analizu punopoljnih mjerenja te otvara prostor za daljnji razvoj metoda namijenjenih boljem razumijevanju termomehaničkih procesa u materijalima i konstrukcijama.